Accepted Manuscript

Anti-methicillin resistant *Staphylococcus aureus* activity, synergism with oxacillin and molecular docking studies of metronidazole-triazole hybrids

Beena Negi, Deepak Kumar, Widuranga Kumbukgolla, Sampath Jayaweera, Prija Ponnan, Ramandeep Singh, Sakshi Agarwal, Diwan S. Rawat

PII: S0223-5234(16)30223-9

DOI: 10.1016/j.ejmech.2016.03.041

Reference: EJMECH 8466

To appear in: *European Journal of Medicinal Chemistry*

Received Date: 21 October 2015

Revised Date: 12 February 2016

Accepted Date: 16 March 2016

Please cite this article as: B. Negi, D. Kumar, W. Kumbukgolla, S. Jayaweera, P. Ponnan, R. Singh, S. Agarwal, D.S. Rawat, Anti-methicillin resistant *Staphylococcus aureus* activity, synergism with oxacillin and molecular docking studies of metronidazole-triazole hybrids, *European Journal of Medicinal Chemistry* (2016), doi: 10.1016/j.ejmech.2016.03.041.

Anti-Methicillin Resistant *Staphylococcus aureus* Activity, Synergism with Oxacillin and Molecular Docking Studies of Metronidazole-Triazole Hybrids

Beena Negi,[†] Deepak Kumar,[†] Widuranga Kumbukgolla,[‡] Sampath Jayaweera,[‡] Prija Ponnan,[†] Ramandeep Singh,[§] Sakshi Agarwal,[§] and Diwan S. Rawat[*†]

[†] Department of Chemistry, University of Delhi, Delhi-110007, India.

[‡] Faculty of Medicine and Allied Sciences, Rajarata University of Sri Lanka, Mihinthale, Sri Lanka

[§] Translational Health Science and Technology Institute, Vaccine and Infectious Disaease Research Centre, Gurgaon-122016, India

Graphical abstract

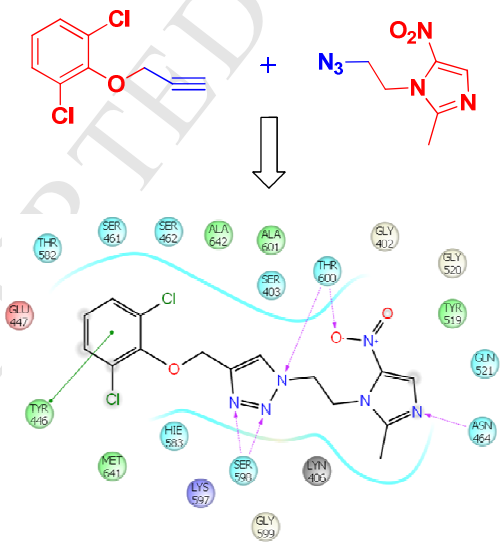

MIC upto 4μg/mL against MRSA

Anti-Methicillin Resistant *Staphylococcus aureus* Activity, Synergism with Oxacillin and Molecular Docking Studies of Metronidazole-Triazole Hybrids

Beena Negi,[†] Deepak Kumar,[†] Widuranga Kumbukgolla,[‡] Sampath Jayaweera,[‡] Prija Poonan,[†] Ramandeep Singh,[§] Sakshi Agarwal,[§] and Diwan S. Rawat[*†]

[†] Department of Chemistry, University of Delhi, Delhi-110007, India.

[‡] Faculty of Medicine and Allied Sciences, Rajarata University of Sri Lanka, Mihinthale, Sri Lanka

[§]Translational Health Science and Technology Institute, Vaccine and Infectious Disaease Research Centre, Gurgaon-122016, India

Abstract

MRSA causes 60-70% of *S. aureus* infection in hospitals and it has developed resistance against the currently available drugs. Interestingly, a series of 35 metronidazole-triazole hybrids on screening against MRSA were found to be active. Compound **22** was found to be effective at 4 µg/mL concentration against nine strains of MRSA. The inhibitory activity was further enhanced upto 1 µg/mL when this compound was used in combination with oxacillin in 1:1 ratio. All the compounds were found to be non-toxic in THP-1 cell line upto a concentration of 50 µM. The time-kill kinetics studies suggested bacteriostatic nature of the compounds. In silico studies show that these compounds interact with Thr600, Ser598, Asn464, His583 and Tyr446 in the active site of PBP2a crystal structure from MRSA.

Key Words: MRSA, Metronidazole, PBP2a, Oxacillin, Triazole, Methicillin, Oxacillin.

*Corresponding author:

E. Mail: dsrawat@chemistry.du.ac.in

Phone No: 91-11-27667465

Fax No: 91-11-27667501

1. Introduction

Staphylococcus aureus is the leading cause of infections in the hospitals worldwide. *Staphylococcus aureus* strains resistant to methicillin were first found in England, in 1961.[1] Since, then the incidences of hospital acquired (HA) and community acquired (CA) methicillin-resistant *Staphylococcus aureus* (MRSA) is ever increasing.[2-7] The number of deaths due to MRSA is near to the total number of deaths due to AIDS, tuberculosis and viral hepatitis all together. Over the years, the semi-synthetic β-lactams such as oxacillin, cloxacillin, flucloxacillin were antibiotics of choice for the treatment of *S. aureus* infections. Besides β-lactam antibiotics, presently other classes of compounds have also been approved by FDA as anti-MRSA agents such as, peptide antibiotics (vancomycin and daptomycin), glycylcyclines (tigecycline), and oxazolidinone class of drugs (linezolid).[8,9] Bouley et al., have recently reported quinazolinones as a promising antibiotic for the treatment of highly resistant MRSA infections.[10] Unfortunately, MRSA has developed resistance to β-lactam antibiotics (penicillin, methicillin, oxacillin, dicloxacillin and ceftaroline), vancomycin and glycopeptides.[11-13] With the emergence of multidrug resistant MRSA, new anti-MRSA therapeutic strategies are needed, especially agents that are orally bioavailable. The rapid evolution of antibiotic resistant bacterial pathogens and the slower pace for the discovery of novel antibiotics, has a devastating effect on the potential for treatment of bacterial infections.[14-16].

When methicillin-susceptible *S. aureus* (MSSA) acquires the methicillin-resistance gene mecA by horizontal gene transfer mediated by staphylococcal cassette chromosome (SCC), MRSA is born.[17,18] The β-lactam antibiotics act by associating with the penicillin binding proteins (PBPs), resulting in the inhibition of the cell wall synthesis, leading to growth inhibition or cell lysis. Resistance to β-lactams emerge if penicillin binding protein 2a (PBP2a) is over expressed by MRSA. Because of the low binding affinity between PBP2a (encoded by the gene mecA) and β-lactams, the cell wall synthesis can be renewed. This protein thus acts as an effective equipment for the MRSA to prevent the attack from β-lactams. The reason for the resistance is credited to the induction of specific genes coding for a monofunctional DD-transpeptidase enzyme penicillin binding protein 2a (PBP2a) by β-lactam exposure.[19] These β-lactam antibiotics irreversibly inhibit PBP2 by acylation of active site serine residue (Ser403),[20] in contrast, the PBP2a of MRSA is resistant to β-lactam acylation and successfully catalyzes the DD-transpeptidation reaction necessary to complete

the cell wall. Recent report highlights the presence of an allosteric site located 60Å distance from the PBP2a active site and it is capable of binding three ligands including one molecule of ceftaroline, muramic acid and peptidoglycan.[21,22] Such allosteric binding triggers conformational changes in PBP2a active site, allowing another inhibitor molecule (ceftaroline) to bind there.[20] Although PBP2a have also developed resistance against ceftaroline in certain strains with mutations (N146K and E150K) observed in allosteric domain and H351N mutation in region away from allosteric and active sites.

Metronidazole (MTZ) and other imidazole derivatives are known for their antibacterial activity.[23-27] The triazole[28] nucleus is a well known pharmacophore for anti-MRSA activity. In continuation with our earlier work on antibacterial agents, we screened the MTZ-triazole hybrids against MRSA.[29-35] These MTZ-triazole hybrids were found to be effective against MRSA strains upto 4 µg/mL concentration. We determined that the MTZ-triazoles can also decrease the minimal inhibitory concentration of oxacillin, many-fold against MRSA. The synergistic activity shows that MTZ-trizoles can be used in combination with oxacillin.

2. Chemistry

Click chemistry has been widely used for the construction of various biologically active molecules due to its ease of synthesis and the possibility of the generation of a library of compounds through various modifications. The copper catalysed azide-alkyne cycloaddition reaction results in the formation of 1,4-disubstituted 1,2,3-triazoles, which are bioisosteres of the amide bond. In the present study, the synthesis of MTZ-triazole hybrids were accomplished in the sequence of reactions as depicted in scheme 1. Various terminal alkynes were synthesized using Williamson ether synthesis starting from various substituted phenols and anilines with propargyl bromide under basic conditions. The hydroxyl group of MTZ was converted to tosylate, an easily leaving group, by reaction of MTZ (**1**) with *p*-toluenesulfonyl chloride (*p*-TsCl) in pyridine (scheme 1). The resulting compound (**2**) on treatment with sodium azide gave 1-(2-azidoethyl)-2-methyl-5-nitro-1*H*-imidazole (**3**). Reactions of compound **3** with terminal alkynes in presence of sodium ascorbate and $CuSO_4.5H_2O$ in *t*-BuOH/H_2O (1:1) (scheme 1) lead to the formation of desired hybrid molecules (**4-38**) in good yield (51-75%). All the compounds were purified over silica gel column. The structures of the compounds were confirmed by various spectroscopic techniques. The absence of characteristic IR peaks for C≡C (alkyne) near 2120 cm^{-1} and for

azido group of compound **3** near 2100 cm^{-1} indicates the formation of triazole. The N=O stretching bands for all the compounds were observed in the region 1502-1599 and 1358-1372 cm^{-1}. In the ^{1}H NMR spectra, the protons of methyl group attached to imidazole ring resonate at about 1.7-2.0 ppm as singlet, the four protons of the ethylene (CH_2CH_2) linker appeared in the region 4.5-5.2 ppm. The imidazole and triazole ring protons appeared as singlets in the region 7.7-8.2 ppm.

<Insert Scheme 1 here>

3. Results and Discussion

The agar plate dilution method was conducted using 35 metronidazole-triazole hybrids against 30 MRSA strains and the MIC of each compound against each MRSA strain was obtained. Table 1 shows the number of MRSA strains against which the compounds are effective at a particular concentration. All the compounds were active against one or another strain of MRSA at 64 µg/mL concentration. Ten compounds (**4, 6, 10, 11, 12, 17, 22, 25, 28** and **31**) were active at 8 µg/mL. Compound **4, 11**, **22, 25** and **28** were active at 4 µg/mL against 1, 3, 9, 1 and 1 strains of MRSA, respectively. Compound **11** with benzene ring linked *via* an ethereal bridge to triazole nucleus exhibited MIC 4 µg/mL against 3 strains of MRSA. In general, compounds having halogen substituents at the benzene nucleus exhibited better activity than the other substituents. Compound **22** with 2,4-dichloro substituent in the phenyl ring was found to be highly active against 9 strains of MRSA at a concentration of 4 µg/mL. Compounds having substituents such as Me, *i*-Pr, *t*-Bu, CHO, NO_2 at the benzene ring were found to be less active. Compounds with NH instead of oxygen atom were also less active than the oxygen linked compounds. Though in these compounds a halogen substituent at 2-position is well tolerated and the compounds **28** and **31** were active at MIC 8 µg/mL.

Compound **22** showed better activity with MIC 4 µg/mL, than oxacillin against 9 strains, whereas oxacillin is effective upto 64 µg/mL. This most active compound **22** was also examined for synergy with the reference drug oxacillin. A mixture of compound **22** and oxacillin was prepared in 1:1 ratio. The concentration of the compound **22** or oxacillin in the mixture was 32 µg/mL. The agar plate dilution method was conducted using the mixture. The study showed that both in combination in ratio 1:1 exhibited promising activity. The activity enhanced upto 1 µg/mL against eleven strains of MRSA. Five strains for which MIC for both oxacillin and compound **22** were >128 or 128 µg/mL, surprisingly showed MIC 2 or 4 µg/mL

when used in combination. Thus it can be concluded that these hybrids have a strong ability to lower the minimal inhibitory concentration (MIC) of a conventional β-lactam, oxacillin.

The synergy between MTZ and oxacillin could be explained by two possible mechanisms; structural modification or altered synthesis of PBP2a. In this study, we have shown the possibility of binding MTZ hybrids to PBP2a in a computational model. This kind of binding can lead to allosteric modification of PBP2A which likely can restore the affinity of PBP2a to oxacillin.[20] Therefore, oxacillin can bind efficiently and inhibit PBP2a which ultimately reduces the cell wall synthesis In a situation of altered synthesis of PBP2a, MTZ can act in DNA level. It is well known that MTZ generate reactive intermediates and those intermediates damage DNA.[36,37] Here, the reactive intermediates can affect the activity of MecA gene altering the synthesis of PBP2a. If PBP2a synthesis reduces, oxacillin can inhibit the cell wall synthesis more efficiently.

<Insert Table 1 here>

<Insert Table 2 here>

The most active compound **22,** at 32 µg/mL concentration was selected for kill kinetics activity (Table 3). The experiment was done in duplicate and the mean value was used to draw the kill kinetics curve (Figure 1). The activity was monitored over 24 hour. The compound **22** inhibited the growth of bacteria entering to the exponential phase resulting nearly constant bacterial counts. Compound **22** and its combination with oxacillin also showed bacteriostatic effects, however, with a slight reduction of colony counts after 14 h; may be due weak cell wall causing the lysis of some bacterial cells. Overall, the time-kill curves indicate that the compounds are bacteriostatic in nature. Further, all the compounds were tested for their toxicity using THP-1 cell line. These cell lines may be used to test the toxicity of the newly synthesized compounds.[38,39] The compounds were found to be non-toxic upto a concentration of 50 µM the highest concentration tested.

<Insert Table 3 here>

<Insert Fig. 1 here>

In the present work, we have attempted to study the interactions of novel MTZ-triazole hybrids with PBP2a structure from MRSA, targeting the PBP2a active site. For this purpose molecular docking studies of some compounds (**4**, **10, 11, 12, 22, 25** and **28**) were performed in the binding pocket of PBP2a crystal structure from MRSA (PDB ID:3ZFZ).

The results of docking studies and the docked conformations of best scored ligands in the active site of PBP2a are shown in table 4 and figures 2 to figure 6. These docking results clearly indicate that the most active compounds exhibited significant binding affinities towards the PBP2a structures (Glide energy range -55.457 kcalmol^{-1} to -40.322 kcalmol^{-1}) and the energy ranges are comparable to that of reference compound oxacillin (Table 4). The compounds showed hydrogen bond interactions along with π-π interactions in the predicted binding poses. Compound **25** having lowest binding energy (-55.457 kcalmol^{-1}) and considerable high Glide XP score (-7.293 kcalmol^{-1}) shows hydrogen bonding interaction between oxygens of nitro group of the compound and side chain atoms of Thr600 and Ser598 of the protein (Figure 5). Another hydrogen bonding interaction is observed between the oxygen atom present in the linker between triazole and naphthalene ring of compound **25** with side chain NH of Asn464. Further π-π interaction between aromatic ring of His583 and Tyr446 of PBP2a and imidazole ring of compound **25** is observed (Figure 5).

<Insert Table 4 here>

Another compound **11**, predicted to have low binding energy (-53.285 kcalmol^{-1}) and high glide score (-6.596 kcalmol^{-1}) and displayed similar H-bonding pattern between oxygens of nitro group substituent in imidazole ring of the compound and side chain atoms of Thr600 and Ser598 of the protein. Hydrogen bonding interaction is also observed between the oxygen atom present in the linker between triazole and benzene ring of compound **11** with side chain NH of Asn464 (Figure 3).

Compound **22** having 2,6-dichloro substitution the benzene ring also show high docking score (-6.323) and low binding energy (-49.945). In the binding pose nitrogen atom of the imidazole ring of compound **22** was found to form a hydrogen bond with OH group of Asn464 side chain (Figure 4). Backbone nitrogen atom of Thr600 is forming two hydrogen bonds, one with oxygen atom of the nitro substituent of imidazole ring and one of the nitrogen atoms of the triazole. Further, OH atom in the side chain of Ser598 forms two hydrogen bonds with the nitrogen atoms of triazole ring of compound **22** (Figure 4).

<Insert Fig. 2 here>

<Insert Fig. 3 here>

<Insert Fig. 4 here>

<Insert Fig. 5 here>

<Insert Fig. 6 here>

The interaction pattern observed for MTZ-triazole hybrids in the active site of PBP2a involves amino acids Thr600, Ser598, Asn464, His583 and Tyr446 that play pivotal roles in the binding of β-lactam antibiotics in the PBP2a active site. Interestingly, none of the MTZ-triazole hybrids have shown to interact with Ser403 which is involved in acylation of β-lactam antibiotics. Such binding mode is reminiscent of the suggestions provided by Lim and Strynadka for designing anti-MRSA drug that could tightly bind non-covalently to PBP2a binding site and is devoid of β-lactam moiety.[40] Hence these observations could be viewed beneficial for developing antibiotics against broadly resistant MRSA strains.

Different pharmacokinetic (PK) parameters for MTZ-triazole hybrids were calculated. The most important of these parameters together with its permissible ranges are listed in the tables S1 and S2. In the present study, most of the test compounds have value for Lipinski's rule of 5 violations less than the maximum permissible value of 4,[41] indicating that these test compounds are endowed with drug likeness properties. Lipinski's rule of 5 is a preliminary test for the drug-likeness of the compounds that require an ideal orally bioactive compound to have no more than 5 and 10 hydrogen bond donors (donorHB) and acceptors (accptHB), respectively, molecular weights (mol_MW) less than 500 amu, and partition coefficients between octanol and water (QPlog P(oct/wat)) less than 5. Most of the MTZ-triazole hybrids in the study show no violation of Lipinski's rule of 5, except for compounds **19** (CH_2OPh-4-NO_2**)**, **24** (CH_2OPh-2,4,6-*t*-Bu) and **36** (NHPh-3,5-OMe) that possess Lipinski's rule of 5 violation of one (Table S1).

Prediction of oral drug absorption (Percent Human Oral Absorption) was highly satisfactory for all the test compounds. It is noteworthy that most of highly active test compounds is predicted to have high percentage (>80%) of Human Oral Absorption as compared to the reference compounds oxacillin, methicillin and metronidazole (Table S2), indicating that MTZ-triazole hybrids could be developed as an orally dosed drug for the treatment of MRSA infection. Studies suggest that the oral bioavailability is influenced by compound's flexibility and can be measured by the number of rotatable bonds (<15) and polar surface area (70 $Å^2$-200 $Å^2$).[42] In the present study, all the test compounds have a number of rotatable bonds (<15) and the polar surface area falls satisfactorily within the permissible range (Table S2). Moreover, molecules possessing values for Lipinski's rule of 5 in permissible ranges could be viewed more likely to have good intestinal absorption or

permeation and is confirmed by the predicted Caco-2 cells permeability (QPPCaco), used as a model for the gut-blood barrier.[43] QPPCaco predictions for all the test compounds showed very good values compared to the β-lactams (oxacillin and methicillin) (Table S2). Further, QPlogKhsa which is the prediction for human serum albumin binding, shows that the predicted values for all the inhibitors lie within the expected range for 95% of known drugs (-1.5 to 1.5). Also, the QikProp descriptor for brain/blood partition coefficient (QPlogBB) show satisfactory predictions for all the test compounds and the reference compounds. Furthermore, QPlogHERG descriptor for the prediction of IC_{50} value of HERG K^+ channel blockage was predicted for the test compounds. Compounds **4** (CH_2Br), **12** (CH_2OCH_3), and **22** (CH_2OPh-2,6-Cl) have been predicted to possess QPlogHERG values in below concern range (< -5) comparable to reference compounds oxacillin, methicillin and metronidazole (Table S2).

4. Conclusions

All the synthesized compounds were found to be effective against MRSA. The best active compound **22** showed good synergism with the reference drug oxacillin. All the compounds were found to be nontoxic up to 50 μM concentration against THP-1 cell line. Also, the compounds exhibited good pharmacokinetic properties and follow the Lipinski's rule of 5. Thus we believe that these compounds can be considered as a possible lead for the development of new anti-MRSA agents.

5. Experimental Protocols

5.1. Biological Activity

5.1.1. *In vitro* anti-MRSA activity

MRSA strains were isolated using axilla and nasal swabs obtained from Medical Students and Patients at Teaching Hospital Anuradhapura, Sri Lanka. After swabbing axilla and nasal areas, the swabs were dipped in NaCl enriched nutrient broth. Following overnight incubation at 37 ^oC, those swabs were streaked on Manitol Salt Agar Plates. The colonies which turned adjacent media into yellow color were selected and the Gram stained smears of those were observed through light microscopy. The cultures which showed Gram positive clusters were followed by coagulase test to identify *S. aureus*. The MIC value of oxacillin against each *S. aureus* strain was determined by agar plate dilution method (Andrews *et al*.) The dilution series was quality controlled using NCTC 6571 *S. aureus* organism. A total

number of 100 strains of MRSA strains were maintained in the culture collection and 30 strains of those were used for experiments.

5.1.1.1. Agar well method: The antibacterial activity of the synthesized compounds was initially screened using agar well method. The bacteria (MRSA) which were obtained from a one day old culture were dissolved in sterile water. And the visual density of the organism was adjusted according to the McFarland-0.5 standard. By soaking a cotton swab in the microbial solution, and streaking the swab on the surface of the Mueller-Hinton agar, a microbial lawn was prepared. A well was dug using the cokeborer (16 mm diameter) in the microbial lawn containing agar plate. The well was filled with the aqueous solution of the compound (1000 µg/mL) using a pasture pipette. The plates were observed for a clear zone around the wells after overnight (24 h) incubation at 37 ^{o}C. The diameter of each clear zone was measured. The compounds which were exhibited a clear zone around the wells, were further subjected for the determination of MIC against 30 MRSA strains using agar plate dilution method.

5.1.1.2. Agar plate dilution method: A dilution series was prepared using anti-bacterial compounds in the concentration range 0.03–128 µg/mL. MRSA was suspended in water using a cotton swab until the visual density equals to McFarland 0.5 standard. The agar plates which contain antibacterial compounds were inoculated using MRSA suspension. The plates were incubated 24 h at 37 ^{o}C and were observed for white colored spots which indicate the growth of the organism. NCTC 6571 *S. aureus* was used to quality control the dilution series.

5.2. Bacterial counts for Time-kill curve

Four separate incubation mixtures containing antibacterial compounds (Oxacillin, MTZ, Compound **22** and the compound **22** with Oxacillin in 1:1 ratio) were prepared in nutrient broth and the control was set without introducing any compound. After adding equal amount of MRSA to each incubation mixture including the control, the final volume was adjusted to 10 mL and the concentration of each antibacterial compound was kept at 32 µg/mL. The initial colony count and subsequent colony counts were obtained using pour plate method, at each 4 h time intervals, over 24 h period. In conducting pour plate technique the bacteria was diluted in the range of 10^{1} to 10^{-7} using nutrient broth. The inoculum (1 mL) which was obtained from each dilution was mixed with melted nutrient agar, separately and poured into separate petri-dishes. The plate which contained 30-300 colonies in prepared

dilution series was used to calculate the colony counts. Same procedure was followed for each mixture of compounds at each time interval.

5.3. *In silico* ADMET prediction

The ADME properties of test compounds and reference compounds (oxacillin, methicillin and metronidazole) are predicted for the pharmaceutically relevant properties to assess the drug likeness and pharmacokinetic properties. The Qikprop v3.5 (Schrödinger, Inc., New York, NY, 2012) was used for the evaluation of some important absorption, distribution, metabolism and elimination (ADME) parameters and its permissible ranges are listed in the Tables 4 and 5.

All the compounds were prepared in neutralized form for the calculation of pharmacokinetic properties by Maestro Build module and LigPrep, saved in SD format. In the present study, the test compounds showed good preliminary test of the druglikeness based on Lipinski's rule of 5 showing zero violation of the rule, proving all the test compounds to be orally active. The descriptor QPPCaco indicating Caco-2 cells permeability, a model used for the gut-blood barrier, showed good values for all the test compounds. Similarly the values of descriptor model such as number of rotatable bond (#rotor) and polar surface area (PSA), used as an indicator of bioavailability for the test compounds lie in expected ranges. Further, the prediction for human serum albumin binding (QPlogKhsa) and QikProp descriptor for brain/blood partition coefficient (QPlogBB) and the blood-brain barrier mimic MDCK cell permeability (QPPMDCK) show satisfactory predictions for all the test compounds (Table S1).

5.4. Molecular docking studies

The 2D structures of all the compounds were generated by drawing on ChemBioDraw Ultra 12.0 (www.cambridgesoft.com). Ligprep module implemented in Schrödinger was used to generate energy minimized 3D structures. Partial atomic charges were computed using the OPLS_2005 force field. The correct Lewis structure, tautomers and ionization states (PH 7.0 +/− 2.0) for each of these ligands were generated and optimized with default settings (Ligprep 2.5, Schrödinger, LLC, New York, NY, 2012). The results of docking studies using Glide XP method could be evaluated using Glide energy and GlideScore XP. Glide Energy is a modified Coulomb-van der Waals interaction energy which is used for comparing binding affinities of different ligands using Charge-dipole and dipole interactions. GlideScore XP

includes XP scoring functions, penalities and XP terms such as Van der Waals energy, Coulomb energy, Lipophilic term, Hydrogen-bonding term, rewards and penalties for various features, such as buried polar groups, hydrophobic enclosure, correlated hydrogen bonds, amide twists, penalty for freezing rotatable bonds, pi-pi stacking reward, reward for pi-cation interactions etc.[44] The 3D crystal structure of PBP2a protein from MRSA (PDB ID:3ZFZ; resolution 2.25 Å), was retrieved from protein data bank (www.rcsb.org). The proteins were prepared for docking using Protein Preparation Wizard (Maestro 10.0 Schrödinger, LLC, New York, NY, 2012). Water molecules within 5 Å of the protein structures was considered. Bond order and formal charges were assigned and hydrogen atoms were added to the crystal structure. Further to refine the structure OPLS-2005 force field parameter was used to alleviate steric clashes and the minimization was terminated when RMSD reached maximum cut-off value of 0.30 Å. The location of co-crystalized ligand Ceftaroline in protein active site was used to choose the center and size of the receptor grid, which was generated using Glide 5.8 (Schrödinger, LLC, New York, NY, 2012) with default settings for all parameters. The grid size was chosen sufficiently large to include all active site residues involved in substrate binding. All ligand conformers were docked to each of the receptor grid files (PfDHFR-TS wild and mutant structures) using Glide extra precision (XP) mode. Default settings were used for the refinement and scoring.

5.5. Materials and methods

All of the chemicals used in the synthesis were purchased from Sigma-Aldrich and were used as such. The progress of the reactions was monitored by using thin layer chromatography (E. Merck Kieselgel 60 F_{254}). Compounds were purified over silica gel (60-120 mesh) column. Meting points were recorded on an ERS automated melting point apparatus and are uncorrected. IR spectra were recorded using Perkin-Elmer and Bruker FT-IR and the values are expressed as λ_{max} cm^{-1}. Mass spectral data were recorded on a Jeol-AccuTOF JMS-T100LC and micromass LCT Mass Spectrometer. ^{1}H NMR and ^{13}C NMR spectral data were recorded on Bruker Spectrospin spectrometer at 300 MHz and 75 MHz and on Jeol ECX spectrospin instrument at 400 and 100 MHz, respectively using $CDCl_3$ and DMSO-d_6 as solvent and TMS as internal reference. The chemical shift values are recorded on δ scale and the coupling constants (*J*) are in Hz.

5.5.1. Typical procedure for the synthesis of metronidazole-triazole conjugates ***(4-38)****:* To a vigorously stirred solution of 1-(2-azido-ethyl)-2-methyl-5-nitro-*1H*-imidazole (**3**), (2.5

mmol) and appropriate alkyne (2.5 mmol) in *tert*-butyl alcohol was added a solution of $CuSO_4.5H_2O$ (0.51 mmol) and sodium ascorbate (1.02 mmol) in distilled water (scheme 1). The amount of *tert*-butyl alcohol and distilled water was kept 1:1 (v/v). The deep yellow mixture was stirred vigorously at room temperature and progress of reaction was monitored by thin layer chromatography. After 2 h, reaction was completed and crude reaction mixture was extracted with $CHCl_3$ (3 × 10 mL) and dried over anhydrous Na_2SO_4. Excess of solvent was removed under vaccum. The crude mixture was purified over SiO_2 column using ethyl acetate/hexane as an eluent.

5.5.2. 4-Bromomethyl-1-[2-(2-methyl-5-nitro-imidazol-1-yl)-ethyl]-1H-[1,2,3]triazole ***(4)*****:** Yield 52%; mp 108-110 ^oC; IR (KBr, cm^{-1}): 3127, 2947, 1526, 1461, 1429, 1369, 1268, 1199, 1117, 1028, 1008; ^1H NMR (300 MHz, DMSO-d_6) δ: 1.83 (s, 3H, CH_3), 3.73 (s, 2H, CH_2Br), 4.59-4.81 (m, 4H, 2NCH_2), 7.95 (s, 1H), 8.03 (s, 1H); ^{13}C NMR (100 MHz, DMSO-d_6) δ: 12.80, 18.91, 24.98, 30.05, 46.25, 48.70, 59.01, 61.26, 96.56, 124.92, 133.25, 138.39, 144.21, 151.21; ESI-MS (*m/z*) calculated for $C_9H_{11}BrN_6O_2$: 314.01, found: 315.10 $[M + H]^+$, 317.11 $[M + 2]^+$; Anal. calcd. for $C_9H_{11}BrN_6O_2$: C, 34.30; H, 3.52; Br, 25.36; N, 26.67; O, 10.15; found: C, 34.33; H, 3.23; Br, 25.55; N, 26.57; O, 10.28.

5.5.3. Propionicacid-1-[2-(2-methyl-5-nitro-imidazol-1-yl)-ethyl]-1H-[1,2,3]triazol-4-ylmethyl ester ***(5)*****:** Yield 58%; mp 116-118 ^oC; IR (KBr, cm^{-1}): 3118, 3073, 2979, 1732, 1530, 1467, 1425, 1372, 1263, 1174, 1143; ^1H NMR (300 MHz, DMSO-d_6) δ: 1.02 (t, J = 6 Hz, 3H, CH_2CH_3), 1.83 (s, 3H, CH_3), 2.32 (q, J = 6 Hz, 2H, CH_2CH_3), 4.68-4.72 (m, 2H, NCH_2), 4.82-4.85 (m, 2H, NCH_2), 5.09 (s, 2H, OCH_2), 8.01 (s, 1H), 8.06 (s, 1H); ESI-MS (*m/z*) calculated for $C_{12}H_{16}N_6O_4$: 308.12, found: 309.21 $[M + H]^+$; Anal. calcd. for $C_{12}H_{16}N_6O_4$: C, 46.75; H, 5.23; N, 27.26; O, 20.76; found: C, 46.01; H, 5.54; N, 27.57; O, 20.28.

5.5.4. 1-(2-(2-Methyl-5-nitro-1H-imidazol-1-yl)ethyl)-4-((tetrahydro-2H-pyran-2-yloxy) methyl)-1H-1,2,3-triazole ***(6)*****:** Yield 60%; IR (KBr, cm^{-1}): 3423, 2931, 2861, 1526, 1461, 1429, 1366, 1267, 1190, 1148, 1018; ^1H NMR (300 MHz, DMSO-d_6) δ: 1.30-1.36 (m, 2H), 1.44 (brs, 2H), 1.55-1.58 (m, 2H), 2.39 (s, 3H, CH3), 3.74-3.82 (m, 1H), 4.37-4.40 (m, 2H), 4.46-4.55 (m, 2H), 4.81-4.83 (m, 2H), 4.92-4.96 (m, 2H), 7.79 (s, 1H), 8.04 (s, 1H); ESI-MS (*m/z*) calculated for $C_{14}H_{20}N_6O_4$: 336.15, found: 337.22 $[M + H]^+$; Anal. calcd. for $C_{14}H_{20}N_6O_4$: C, 49.99; H, 5.99; N, 24.99; O, 19.03; found: C, 50.22; H, 5.73; N, 25.51; O, 19.28.

5.5.5. 1-(2-(2-Methyl-5-nitro-1H-imidazol-1-yl)ethyl)-4-(trimethylsilyl)-1H-1,2,3-triazole ***(7)*****:** Yield 60%; mp 189-191 ^{o}C; ^{1}H NMR (300 MHz, DMSO-d_6): 0.20 (s, 9H, Si(CH_3)$_3$), 1.54 (s, 3H, CH_3), 4.47 (t, J = 4.2 Hz, 2H, NCH_2), 4.62 (t, J = 4.5 Hz, 2H, NCH_2), 7.72 (s, 1H), 7.83 (s, 1H); ESI-MS (*m/z*) calculated for $C_{11}H_{18}N_6O_2Si$: 294.12, found: 295.31 $[M + H]^+$; Anal. calcd. for $C_{11}H_{18}N_6O_2Si$: C, 44.88; H, 6.16; N, 28.55; O, 10.87; Si, 9.54; found: C, 45.01; H, 6.23; N, 28.87; O, 10.68; Si, 9.77.

5.5.6. 1-(2-(2-Methyl-5-nitro-1H-imidazol-1-yl)ethyl)-4-propyl-1H-1,2,3-triazole ***(8)*****:** Yield 75%; mp 121-122 ^{o}C; IR (film, cm^{-1}): 3123, 2961, 2910, 2861, 1525, 1461, 1370, 1266, 1199, 1148, 1050, 827, 748; ^{1}H NMR (400 MHz, $CDCl_3$) δ: 0.82 (t, J = 7.63 Hz, 3H, $CH_2CH_2CH_3$), 1.49 (sextet, J = 7.63 Hz, 2H, $CH_2CH_2CH_3$), 1.78 (s, 3H, CH_3), 2.49 (t, J = 7.63 Hz, 2H, $CH_2CH_2CH_3$), 4.63-4.66 (m, 2H, NCH_2CH_2N), 4.72-4.75 (m, 2H, NCH_2CH_2N), 7.65 (s, 1H), 8.01 (s, 1H); ^{13}C NMR (100 MHz, $CDCl_3$) δ: 13.30, 13.64, 22.70, 27.39, 46.68, 49.39, 121.55, 133.82, 149.11, 151.42; ESI-MS (*m/z*) calculated for $C_{11}H_{16}N_6O_2$: 264.13, found: 265.24 $[M + H]^+$.; Anal. calcd. for $C_{11}H_{16}N_6O_2$: C, 49.99; H, 6.10; N, 31.80; O, 12.11; found: C, 50.14; H, 6.33; N, 32.09; O, 12.37.

5.5.7. 1-(1-(2-(2-Methyl-5-nitro-1H-imidazol-1-yl)ethyl)-1H-1,2,3-triazol-4-yl)cyclohexanol ***(9)*****:** Yield 68%; mp 151-152 ^{o}C; IR (KBr, cm^{-1}): 3394, 2933, 1533, 1459, 1371, 1265, 1197, 1146, 1049, 826; ^{1}H NMR (300 MHz, DMSO-d_6): 1.33-1.37 (m, 1H), 1.50-1.59 (m, 3H), 1.61-1.80 (m, 6H), 1.94 (s, 3H, CH_3), 2.28 (s, 1H, *OH*), 4.78 (s, 4H, NCH_2CH_2N), 7.10 (s, 1H), 8.0 (s, 1H); ESI-MS (*m/z*) calculated for $C_{14}H_{20}N_6O_3$: 320.15, found: 321.21 $[M + H]^+$; Anal. calcd. for $C_{14}H_{20}N_6O_3$: C, 52.49; H, 6.29; N, 26.23; O, 14.98; found: C, 52.76; H, 6.51; N, 26.48; O, 15.20.

5.5.8. 1-[2-(2-Methyl-5-nitro-imidazol-1-yl)-ethyl]-4-phenyl-1H-[1,2,3]triazole ***(10)*****:** Yield 59%; mp 178-180 ^{o}C; IR (KBr, cm^{-1}): 3124, 1527, 1460, 1367, 1263, 1192, 1149, 1082, 825, 771; ^{1}H NMR (300 MHz, DMSO-d_6) δ: 1.92 (s, 3H, CH_3), 4.77 (brs, 2H, NCH_2), 4.88 (brs, 2H, NCH_2), 7.31-7.36 (m, 3H, Ar*H*), 7.75-7.77 (m, 2H, Ar*H*), 8.06 (s, 1H), 8.43 (s, 1H); ESI-MS (*m/z*) calculated for $C_{14}H_{14}N_6O_2$: 298.11, found: 298.30 $[M]^+$; Anal. calcd. for $C_{14}H_{14}N_6O_2$: C, 56.37; H, 4.73; N, 28.17; O, 10.73; found: C, 55.99; H, 4.52; N, 28.42; O, 10.95.

5.5.9. 1-[2-(2-Methyl-5-nitro-imidazol-1-yl)-ethyl]-4-phenoxymethyl-1H-[1,2,3]triazole ***(11)*****:** Yield 54%; mp 146-148 ^{o}C; IR (KBr, cm^{-1}): 3128, 2932, 1527, 1466, 1428, 1367, 1252, 1196, 1151, 1049, 884; ^{1}H NMR (300 MHz, DMSO-d_6) δ: 1.80 (s, 3H, CH_3), 4.71 (t, J = 5.4

Hz, 2H, NCH_2), 4.85 (t, J = 5.4 Hz, 2H, NCH_2), 5.12 (s, 2H, OCH_2), 6.92-7.01 (m, 3H, Ar*H*), 7.26-7.31 (m, 2H, Ar*H*), 8.04 (s, 1H), 8.11 (s, 1H); ^{13}C NMR (100 MHz, DMSO-d_6) δ: 12.74, 46.21, 48.78, 60.77, 114.70, 120.85, 125.34, 129.50, 133.28, 138.37, 143.17, 151.23, 157.86; ESI-MS (*m/z*) calculated for $C_{15}H_{16}N_6O_3$: 328.12, found: 329.23 $[M + H]^+$; Anal. calcd. for $C_{15}H_{16}N_6O_3$: C, 54.87; H, 4.91; N, 25.60; O, 14.62; found: C, 54.99; H, 5.14; N, 25.82; O, 14.45.

5.5.10. 1-[2-(2-Methyl-5-nitro-imidazol-1-yl)-ethyl]-4-o-tolyloxymethyl-1H-[1,2,3]triazole ***(12)*****:** Yield 60%; mp 134-136 ^{o}C; IR (KBr, cm^{-1}): 3128, 2924, 2854, 1526, 1461, 1430, 1268, 1243, 1193, 1120, 1052, 1006; ^{1}H NMR (300 MHz, DMSO-d_6) δ: 1.74 (s, 3H, CH_3), 2.09 (s, 3H, CH_3), 4.69-4.71 (m, 2H, NCH_2), 4.83-4.85 (m, 2H, NCH_2), 5.10 (s, 2H, OCH_2), 6.81-6.86 (m, 1H, Ar*H*), 7.03-7.06 (m, 1H, Ar*H*), 7.11-7.13 (m, 2H, Ar*H*), 8.03 (s, 1H), 8.08 (s, 1H); ^{13}C NMR (100 MHz, DMSO-d_6) δ: 12.82, 46.24, 48.73, 57.10, 64.71, 124.85, 133.27, 138.39, 144.14, 151.23; ESI-MS (*m/z*) calculated for $C_{16}H_{18}N_6O_3$: 342.14, found: 343.19 $[M + H]^+$; Anal. calcd. for $C_{16}H_{18}N_6O_3$: C, 56.13; H, 5.30; N, 24.55; O, 14.02; found: C, 56.44; H, 5.67; N, 24.79; O, 14.31.

5.5.11. 1-[2-(2-Methyl-5-nitro-imidazol-1-yl)-ethyl]-4-p-tolyloxymethyl-1H-[1,2,3]triazole ***(13)*****:** Yield 52%; mp 142-143 ^{o}C; IR (KBr, cm^{-1}): 2924, 2854, 1538, 1509, 1465, 1369, 1266, 1235, 1190, 1155, 1047; ^{1}H NMR (300 MHz, DMSO-d_6) δ: 1.78 (s, 3H, CH_3), 2.21 (s, 3H, CH_3), 4.70 (brs, 2H, NCH_2), 4.82 (brs, 2H, NCH_2), 5.05 (s, 2H, OCH_2), 6.85 (d, J = 8 Hz, 2H, Ar*H*), 7.05 (d, J = 8 Hz, 2H, Ar*H*), 8.02 (s, 1H), 8.07 (s, 1H); ^{13}C NMR (75.5 MHz, DMSO-d_6): 12.73, 20.05, 48.73, 60.87, 114.56, 125.23, 129.49, 129.78, 133.23, 138.34, 143.26, 151.19, 155.74; ESI-MS (*m/z*) calculated for $C_{16}H_{18}N_6O_3$: 342.14, found: 343.22 $[M + H]^+$; Anal. calcd. for $C_{16}H_{18}N_6O_3$: C, 56.13; H, 5.30; N, 24.55; O, 14.02; found: C, 56.47; H, 5.61; N, 24.69; O, 14.24.

5.5.12. 4-((4-iso-Propylphenoxy)methyl)-1-(2-(2-methyl-5-nitro-1H-imidazol-1-yl)ethyl)-1H-1,2,3-triazole ***(14)*****:** Yield 62%; mp 147-149 ^{o}C; IR (KBr, cm^{-1}): 3131, 2958, 2924, 1747, 1700, 1650, 1611, 1511, 1430, 1364, 1264, 1241, 1191, 1147; ^{1}H NMR (300 MHz, $CDCl_3$) δ: 1.12 (d, J = 6.87 Hz, 6H, CH(CH_3)$_2$), 1.74 (s, 3H, CH_3), 2.78 (septet, J = 6.87 Hz, 1H, CH(CH_3)$_2$), 4.65-4.68 (m, 2H, N$CH_2$$CH_2$$NH_2$), 4.79-4.82 (m, 2H, N$CH_2$$CH_2$$NH_2$), 5.04 (s, 2H, O$CH_2$), 6.86 (d, J = 8.39 Hz, 2H, Ar*H*), 7.10 (d, J = 8.39 Hz, 2H, Ar*H*), 8.01 (s, 1H), 8.06 (s, 1H); ^{13}C NMR (100 MHz, DMSO-d_6) δ: 12.73, 24.11, 32.60, 36.21, 48.77, 60.88, 114.53, 125.26, 127.14, 133.27, 138.37, 140.73, 143.34, 151.23, 155.96; ESI-MS (*m/z*)

calculated for $C_{18}H_{22}N_6O_3$: 370.17, found: 371.24 $[M + H]^+$; Anal. calcd. for $C_{18}H_{22}N_6O_3$: C, 58.37; H, 5.99; N, 22.69; O, 12.96; found: C, 58.68; H, 6.22; N, 22.84; O, 13.09.

5.5.13. 4-((4-tert-Butylphenoxy)methyl)-1-(2-(2-methyl-5-nitro-1H-imidazol-1-yl)ethyl)-1H-1,2,3-triazole ***(15)*****:** Yield 64%; mp 141-142 ^oC; IR (film, cm^{-1}): 3135, 3108, 2962, 2868, 1608, 1527, 1513, 1466, 1429, 1363, 1260, 1244, 1188, 1148; ^1H NMR (300 MHz, $CDCl_3$) δ: 1.20 (s, 9H, $(CH_3)_3$), 1.73 (s, 3H, CH_3), 4.66-4.68 (m, 2H, $NCH_2CH_2NH_2$), 4.79-4.82 (m, 2H, $NCH_2CH_2NH_2$), 5.05 (s, 2H, OCH_2), 6.86 (d, J = 8.39 Hz, 2H, Ar*H*), 7.24 (d, J = 8.39 Hz, 2H, Ar*H*), 8.01 (s, 1H), 8.06 (s, 1H); ^{13}C NMR (100 MHz, DMSO-d_6) δ: 12.73, 31.30, 33.76, 46.23, 48.77, 60.84, 114.18, 125.24, 126.06, 133.27, 142.97, 143.35, 155.60; ESI-MS (*m/z*) calculated for $C_{19}H_{24}N_6O_3$: 384.19, found: 385.26 $[M + H]^+$; Anal. calcd. for $C_{19}H_{24}N_6O_3$: C, 59.36; H, 6.29; N, 21.86; O, 12.49; found: C, 59.22; H, 6.51; N, 22.01; O, 12.86.

5.5.14. 2-{1-[2-(2-Methyl-5-nitro-imidazol-1-yl)-ethyl]-1H-[1,2,3]triazol-4-ylmethoxy}-benzaldehyde ***(16)*****:** Yield 60%; mp 180-182 ^oC; IR (KBr, cm^{-1}): 3141, 3031, 2870, 1679, 1599, 1534, 1475, 1370, 1261, 1241, 1187, 1049, 1004; ^1H NMR (300 MHz, DMSO-d_6) δ: 1.78 (s, 3H, CH_3), 4.72 (brs, 2H, NCH_2), 4.87 (brs, 2H, NCH_2), 5.33 (s, 2H, OCH_2), 7.08-7.13 (m, 1H, Ar*H*), 7.38-7.41 (m, 1H, Ar*H*), 7.65-7.72 (m, 2H, Ar*H*), 8.04 (s, 1H), 8.19 (s, 1H), 10.33 (s, 1H, *CHO*); ^{13}C NMR (100 MHz, DMSO-d_6) δ: 12.68, 46.23, 48.89, 61.85, 114.06, 121.12, 124.43, 125.56, 127.60, 133.26, 136.36, 138.36, 142.69, 151.17, 160.25, 189.10; ESI-MS (*m/z*) calculated for $C_{16}H_{16}N_6O_4$: 356.12, found: 356.17 $[M]^+$; Anal. calcd. for $C_{16}H_{16}N_6O_4$: C, 53.93; H, 4.53; N, 23.58; O, 17.96; found: C, 54.11; H, 4.75; N, 23.78; O, 18.25.

5.5.15. 4-{1-[2-(2-Methyl-5-nitro-imidazol-1-yl)-ethyl]-1H-[1,2,3]triazol-4-ylmethoxy}-benzaldehyde ***(17)*****:** Yield 60%; mp 170-172 ^oC; IR (KBr, cm^{-1}): 2924, 2854, 1683, 1601, 1577, 1524, 1454, 1370, 1261, 1221, 1172, 826; ^1H NMR (300 MHz, DMSO-d_6) δ: 1.77 (s, 3H, CH_3), 4.68-4.71 (m, 2H, $NCH_2CH_2NH_2$), 4.83-4.86 ($NCH_2CH_2NH_2$), 5.25 (s, 2H, OCH_2), 7.18 (d, J = 8.39 Hz, 2H, Ar*H*), 7.85 (d, J = 8.39 Hz, 2H, Ar*H*), 8.03 (s, 1H), 8.14 (s, 1H), 9.86 (s, 1H, *CHO*); ^{13}C NMR (75.5 MHz, DMSO-d_6): 12.68, 46.10, 48.77, 61.19, 115.19, 125.61, 129.82, 131.73, 133.16, 138.32, 142.41, 151.15, 162.73, 191.31; ESI-MS (*m/z*) calculated for $C_{16}H_{16}N_6O_4$: 356.12, found: 357.18 $[M + H]^+$; Anal. calcd. for $C_{16}H_{16}N_6O_4$: C, 53.93; H, 4.53; N, 23.58; O, 17.96; found: C, 54.06; H, 4.62; N, 23.85; O, 18.17.

5.5.16. 4-(2-Chloro-phenoxymethyl)-1-[2-(2-methyl-5-nitro-imidazol-1-yl)-ethyl]-1H-[1,2,3] triazole ***(18)*****:** Yield 63%; mp 140-142 ^{o}C; IR (KBr, cm^{-1}): 3133, 2924, 1525, 1501, 1460, 1430, 1366, 1264, 1195, 1037; ^{1}H NMR (300 MHz, $CDCl_3$) δ: 1.98 (s, 3H, *CH*$_3$), 4.79 (s, 4H, N*CH*$_2$*CH*$_2$N), 5.15 (s, 2H, O*CH*$_2$), 6.66-6.69 (m, 1H, Ar*H*), 6.74-6.75 (m, 1H, Ar*H*), 7.01-7.04 (d, *J* = 8.4 Hz, 1H, Ar*H*), 7.33 (s, 1H), 8.00 (s, 1H); ^{13}C NMR (100 MHz, DMSO-*d*$_6$) δ: 12.73, 18.44, 19.64, 46.21, 48.76, 60.83, 111.67, 116.11, 125.20, 128.33, 130.15, 133.28, 137.29, 138.37, 143.38, 151.22, 155.98; ESI-MS (*m/z*) calculated for $C_{15}H_{15}ClN_6O_3$: 362.08, found: 363.12 $[M + H]^+$, 365.35 $[M + 2]^+$; Anal. calcd. for $C_{15}H_{15}ClN_6O_3$: C, 49.66; H, 4.17; Cl, 9.77; N, 23.17; O, 13.23; found: C, 49.59; H, 4.33; Cl, 10.00; N, 23.38; O, 13.54.

5.5.17. 1-[2-(2-Methyl-5-nitro-imidazol-1-yl)-ethyl]-4-(4-nitro-phenoxymethyl)-1H-[1,2,3]triazole ***(19)*****:** Yield 54%; mp 196-198 ^{o}C; IR (KBr, cm^{-1}): 3127, 2916, 1593, 1502, 1457, 1361, 1259, 1186, 1044, 1106; ^{1}H NMR (300 MHz, $CDCl_3$) δ: 1.99 (s, 3H, *CH*$_3$), 4.82 (brs, 4H, N*CH*$_2$*CH*$_2$N), 5.26 (s, 2H, O*CH*$_2$), 7.04 (d, *J* = 9 Hz, 2H, Ar*H*), 7.36 (s, 1H), 8.00 (s, 1H), 8.21 (d, *J* = 9 Hz, 2H, Ar*H*); ESI-MS (*m/z*) calculated for $C_{15}H_{15}N_7O_5$: 373.11, found: 373.15 $[M]^+$; Anal. calcd. for $C_{15}H_{15}N_7O_5$: C, 48.26; H, 4.05; N, 26.26; O, 21.43; found: C, 48.42; H, 4.25; N, 26.47; O, 21.60.

5.5.18. 4-((2,3-Dimethylphenoxy)methyl)-1-(2-(2-methyl-5-nitro-1H-imidazol-1-yl)ethyl)-1H-1,2,3-triazole ***(20)*****:** Yield 58%; mp 144-146 ^{o}C; IR (film, cm^{-1}): 3128, 2923, 1703, 1656, 1584, 1525, 1461, 1429, 1372, 1269, 1251, 1198, 1093; ^{1}H NMR (300 MHz, $CDCl_3$) δ: 1.95 (s, 3H, *CH*$_3$), 2.11 (s, 3H, *CH*$_3$), 2.30 (s, 3H, *CH*$_3$), 4.81 (s, 4H, N*CH*$_2$*CH*$_2$N), 5.16 (s, 2H, O*CH*$_2$), 6.76-6.82 (m, 2H, Ar*H*), 7.02-7.07 (m, 1H, Ar*H*), 7.30 (s, 1H), 8.0 (s, 1H); ^{13}C NMR (100 MHz, DMSO-*d*$_6$) δ: 11.46, 12.66, 19.73, 46.31, 48.82, 61.39, 109.63, 122.38, 124.34, 125.13, 125.85, 133.28, 137.34, 138.37, 143.61, 151.20, 155.80; ESI-MS (*m/z*) calculated for $C_{17}H_{20}N_6O_3$: 356.15, found: 357.20 $[M + H]^+$; Anal. calcd. for $C_{17}H_{20}N_6O_3$: C, 57.29; H, 5.66; N, 23.58; O, 13.47; found: C, 57.46; H, 5.80; N, 23.72; O, 13.66.

5.5.19. 4-((2,4-Dichlorophenoxy)methyl)-1-(2-(2-methyl-5-nitro-1H-imidazol-1-yl)ethyl)-1H-1,2,3-triazole ***(21)*****:** Yield 67%; mp 120-121 ^{o}C; IR (film, cm^{-1}): 3133, 2941, 1695, 1529, 1472, 1366, 1260, 1191, 1146, 1056, 997, 809; ^{1}H NMR (300 MHz, DMSO-*d*$_6$) δ: 1.72 (s, 3H, *CH*$_3$), 4.65-4.68 (m, 2H, N*CH*$_2$CH$_2$NH$_2$), 4.81-4.83 (t, 2H, NCH$_2$*CH*$_2$NH$_2$), 5.20 (s, 2H, O*CH*$_2$), 7.28-7.35 (m, 2H, Ar*H*), 7.53-7.54 (m, 1H, Ar*H*), 8.00 (s, 1H), 8.10 (s, 1H); ^{13}C NMR (100 MHz, DMSO-*d*$_6$) δ: 12.69, 46.27, 48.87, 62.04, 115.49, 122.48, 124.79, 125.74, 128.01, 129.34, 133.27, 138.36, 142.34, 151.17, 152.34; ESI-MS (*m/z*) calculated for

$C_{15}H_{14}Cl_2N_6O_3$: 396.05, found: 397.11 $[M + H]^+$, 399.18 $[M + 2]^+$, 401.20 $[M + 4]^+$; Anal. calcd. for $C_{15}H_{14}Cl_2N_6O_3$: C, 45.36; H, 3.55; Cl, 17.85; N, 21.16; O, 12.08; found: C, 45.55; H, 3.71; Cl, 17.93; N, 21.30; O, 12.29.

5.5.20. 4-((2,6-Dichlorophenoxy)methyl)-1-(2-(2-methyl-5-nitro-1H-imidazol-1-yl)ethyl)-1H-1,2,3-triazole ***(22)*****:** Yield 68%; mp 170-171 °C; IR (film, cm^{-1}): 3211, 2957, 1696, 1530, 1459, 1365, 1258, 1191, 1146, 1044, 968, 755; ^{1}H NMR (300 MHz, DMSO-d_6) δ: 1.93 (s, 3H, CH_3), 4.79 (t, J = 5.7 Hz, 2H, NCH_2), 4.94 (t, J = 5.7 Hz, 2H, NCH_2), 5.15 (s, 2H, OCH_2), 7.28 (d, J = 8.1 Hz, 1H, Ar*H*), 7.56 (d, J = 8.1 Hz, 2H, Ar*H*), 8.12 (s, 1H), 8.29 (s, 1H); ^{13}C NMR (100 MHz, DMSO-d_6) δ: 12.92, 46.16, 48.76, 65.94, 126.07, 126.32, 128.76, 129.28, 133.27, 138.40, 142.39, 150.17, 151.28; ESI-MS (*m/z*) calculated for $C_{15}H_{14}Cl_2N_6O_3$: 396.05, found: 397.15 $[M + H]^+$, 399.18 $[M + 2]^+$, 401.18 $[M + 4]^+$; Anal. calcd. For $C_{15}H_{14}Cl_2N_6O_3$: C, 45.36; H, 3.55; Cl, 17.85; N, 21.16; O, 12.08; found: C, 45.49; H, 3.67; Cl, 17.91; N, 21.52; O, 12.16.

5.5.21. 4-(Benzyloxymethyl)-1-(2-(2-methyl-5-nitro-1H-imidazol-1-yl)ethyl)-1H-1,2,3-triazole ***(23)*****:** Yield 58%; mp 104-106 °C; IR (film, cm^{-1}): 3189, 2922, 1715, 1530, 1464, 1364, 1263, 1189, 1145, 1049, 823; ^{1}H NMR (300 MHz, DMSO-d_6) δ: 1.88 (s, 3H, CH_3), 4.48-4.56 (m, 4H, 2NCH_2), 4.75-4.87 (m, 4H, 2OCH_2), 7.36 (brs, 5H, Ar*H*), 8.06 (s, 2H); ESI-MS (*m/z*) calculated for $C_{16}H_{18}N_6O_3$: 342.14, found: 343.19 $[M + H]^+$; Anal. calcd. for $C_{16}H_{18}N_6O_3$: C, 56.13; H, 5.30; N, 24.55; O, 14.02; found: C, 56.44; H, 5.52; N, 24.70; O, 14.28.

5.5.22. 1-(2-(2-Methyl-5-nitro-1H-imidazol-1-yl)ethyl)-4-((2,4,6-tri-tert-butylphenoxy)methyl)-1H-1,2,3-triazole ***(24)*****:** Yield 77%; mp 199-200 °C; IR (film, cm^{-1}): 3125, 2960, 1718, 1531, 1468, 1364, 1214, 1176, 1052, 746; ^{1}H NMR (300 MHz, DMSO-d_6) δ: 1.29 (s, 9H, $(CH_3)_3$), 1.38 (s, 18H, 2$(CH_3)_3$), 1.83 (s, 3H, CH_3), 4.75 (s, 4H, 2NCH_2), 4.91 (s, 2H, OCH_2), 7.25 (s, 2H, Ar*H*), 8.07 (s, 1H), 8.13 (s, 1H); ESI-MS (*m/z*) calculated for $C_{27}H_{40}N_6O_3$: 496.31, found: 497.38 $[M + H]^+$; Anal. calcd. for $C_{27}H_{40}N_6O_3$: C, 65.30; H, 8.12; N, 16.92; O, 9.66; found: C, 65.48; H, 8.66; N, 17.12; O, 9.81.

5.5.23. 1-(2-(2-Methyl-5-nitro-1H-imidazol-1-yl)ethyl)-4-((naphthalen-1-yloxy)methyl)-1H-1,2,3-triazole ***(25)*****:** Yield 60%; mp 168-169 °C; IR (film, cm^{-1}): 3127, 2916, 1577, 1524, 1459, 1429, 1371, 1267, 1238, 1198, 1096, 1052; ^{1}H NMR (300 MHz, DMSO-d_6) δ: 1.87 (s, 3H, CH_3), 4.80-4.81 (m, 2H, NCH_2), 4.94 (s, 2H, NCH_2), 5.37 (s, 2H, OCH_2), 7.19 (d, J = 7.2 Hz, 1H, Ar*H*), 7.48-7.56 (m, 4H), 7.93 (d, J = 6.9 Hz, 1H), 8.12-8.15 (m, 2H), 8.27 (s, 1H);

ESI-MS (*m/z*) calculated for $C_{19}H_{18}N_6O_3$: 378.14, found: 379.19 $[M + H]^+$; Anal. calcd. for $C_{19}H_{18}N_6O_3$: C, 60.31; H, 4.79; N, 22.21; O, 12.69; found: C, 60.52; H, 4.96; N, 22.55; O, 12.83.

5.5.24. N-((1-(2-(2-Methyl-5-nitro-1H-imidazol-1-yl)ethyl)-1H-1,2,3-triazol-4-yl)methyl) aniline ***(26)*****:** Yield 62%; mp 137-138 ^oC; IR (KBr, cm^{-1}): 3132, 2958, 2928, 2869, 1611, 1583, 1525, 1510, 1461, 1431, 1371, 1268, 1241, 1198, 1176, 1150, 1116, 1051, 1006, 884, 862; ^1H NMR (300 MHz, DMSO-d_6) δ: 1.79 (s, 3H, CH_3), 3.30 (s, 1H, *NH*), 4.70-4.71 (m, 2H, NCH_2), 4.82-4.83 (m, 2H, NCH_2), 5.07 (s, 2H, CH_2NH), 6.90 (d, *J* = 7.8 Hz, 3H), 7.07 (d, *J* = 7.8 Hz, 2H, Ar*H*), 8.03 (s, 1H), 8.08 (s, 1H); ^{13}C NMR (100 MHz, DMSO-d_6) δ: 12.74, 13.59, 24.34, 36.39, 46.21, 48.78, 60.86, 114.48, 125.27, 129.22, 133.27, 134.40, 138.37, 143.33, 151.21, 155.97; ESI-MS (*m/z*) calculated for $C_{15}H_{17}N_7O_2$: 327.14, found: 327.18 $[M]^+$; Anal. calcd. for $C_{15}H_{17}N_7O_2$: C, 55.04; H, 5.23; N, 29.95; O, 9.78; found: C, 55.31; H, 5.42; N, 30.15; O, 10.01.

5.5.25. 2-Methyl-N-((1-(2-(2-methyl-5-nitro-1H-imidazol-1-yl)ethyl)-1H-1,2,3-triazol-4-yl)methyl) aniline ***(27)*****:** Yield 58%; mp 151-152 ^oC; IR (nujol, cm^{-1}): 3111, 3074, 2924, 2855, 1604, 1523, 1459, 1367, 1314, 1258, 1188, 1050, 742; ^1H NMR (300 MHz, DMSO-d_6) δ: 1.72 (s, 3H, CH_3), 2.05 (s, 3H, CH_3), 4.30 (d, *J* = 5.7 Hz, 2H, CH_2NH), 4.60-4.65 (m, 2H, NCH_2), 4.75-4.76 (m, 2H, NCH_2), 5.40 (t, *J* = 5.7 Hz, 1H, CH_2NH), 6.44-6.47 (m, 2H, Ar*H*), 6.91-6.93 (m, 2H, Ar*H*), 7.76 (s, 1H), 7.99 (s, 1H); ESI-MS (*m/z*) calculated for $C_{16}H_{19}N_7O_2$: 341.16, found: 341.13 $[M]^+$; Anal. calcd. for $C_{16}H_{19}N_7O_2$: C, 56.29; H, 5.61; N, 28.72; O, 9.37; found: C, 56.52; H, 5.90; N, 28.88; O, 9.60.

5.5.26. 2-Fluoro-N-((1-(2-(2-methyl-5-nitro-1H-imidazol-1-yl)ethyl)-1H-1,2,3-triazol-4-yl)methyl) aniline ***(28)*****:** Yield 65%; mp 110-111 ^oC; IR (KBr, cm^{-1}): 3368, 3106, 2858, 1623, 1527, 1461, 1365, 1332, 1294, 1265, 1191, 1153, 1115, 1051, 823; ^1H NMR (300 MHz, DMSO-d_6) δ: 1.72 (s, 3H, CH_3), 4.33 (d, *J* = 6 Hz, 2H, CH_2NH), 4.65 (t, *J* = 5.1 Hz, 2H, NCH_2), 4.78 (t, *J* = 5.1 Hz, 2H, NCH_2), 5.97 (t, *J* = 6 Hz, 1H, *NH*), 6.53-6.55 (m, 1H, Ar*H*), 6.64 (t, *J* = 8.1 Hz, 1H, Ar*H*), 6.91 (t, *J* = 7.8 Hz, 1H, Ar*H*), 6.99 (dd, *J* = 7.8, 4.2 Hz, 1H, Ar*H*), 7.83 (s, 1H), 8.01 (s, 1H); ESI-MS (*m/z*) calculated for $C_{15}H_{16}FN_7O_2$: 345.13, found: 345.09 $[M]^+$; Anal. calcd. for $C_{15}H_{16}FN_7O_2$: C, 52.17; H, 4.67; F, 5.50; N, 28.39; O, 9.27; found: C, 52.29; H, 4.80; F, 5.72; N, 28.54; O, 9.41.

5.5.27. 3-Fluoro-N-((1-(2-(2-methyl-5-nitro-1H-imidazol-1-yl)ethyl)-1H-1,2,3-triazol-4-yl)methyl) aniline ***(29)*****:** Yield 55%; mp 139-140 ^oC; IR (film, cm^{-1}): 3384, 3121, 3021, 1617,

1526, 1464, 1363, 1261, 1187, 1147, 1046, 925, 823, 752; ^{1}H NMR (400 MHz, $CDCl_3$) δ: 1.94 (s, 3H, *CH*$_3$), 4.33 (brs, 1H, *NH*), 4.40 (s, 2H, *CH*$_2$NH), 4.77 (s, 4H, N*CH*$_2$*CH*$_2$N), 6.27-6.31 (m, 1H, Ar*H*), 6.37 (dd, *J* = 8.0, 1.5 Hz, 1H, Ar*H*), 6.40-6.45 (m, 1H, Ar*H*), 7.07-7.13 (m, 1H, Ar*H*), 7.15 (s, 1H), 7.97 (s, 1H); ESI-MS (*m/z*) calculated for $C_{15}H_{16}FN_7O_2$: 345.13, found: 346.19 $[M + H]^+$; Anal. calcd. for $C_{15}H_{16}FN_7O_2$: C, 52.17; H, 4.67; F, 5.50; N, 28.39; O, 9.27; found: C, 52.33; H, 4.82; F, 5.73; N, 28.76; O, 9.43.

5.5.28. 4-Fluoro-N-((1-(2-(2-methyl-5-nitro-1H-imidazol-1-yl)ethyl)-1H-1,2,3-triazol-4-yl)methyl) aniline ***(30)*****:** Yield 57%; mp 138-139 ^{o}C; IR (KBr, cm^{-1}): 3375, 3160, 3113, 3033, 2838, 1612, 1558, 1528, 1510, 1460, 1363, 1262, 1220, 1191, 1155, 1114, 1051; ^{1}H NMR (400 MHz, $CDCl_3$) δ: 1.92 (s, 3H, *CH*$_3$), 4.11 (brs, 1H, *NH*), 4.37 (s, 2H, *CH*$_2$NH), 4.76 (s, 4H, N*CH*$_2$*CH*$_2$N), 6.53-6.56 (m, 2H, Ar*H*), 6.86-6.90 (m, 2H, Ar*H*), 7.13(s, 1H), 7.97 (s, 1H); ESI-MS (*m/z*) calculated for $C_{15}H_{16}FN_7O_2$: 345.13, found: 346.20 $[M + H]^+$; Anal. calcd. for $C_{15}H_{16}FN_7O_2$: C, 52.17; H, 4.67; F, 5.50; N, 28.39; O, 9.27; found: C, 52.30; H, 4.59; F, 5.72; N, 28.68; O, 9.50.

5.5.29. 2-Chloro-N-((1-(2-(2-methyl-5-nitro-1H-imidazol-1-yl)ethyl)-1H-1,2,3-triazol-4-yl)methyl) aniline ***(31)*****:** Yield 59%; mp 146-142 ^{o}C; IR (nujol, cm^{-1}): 3380, 3110, 3033, 2924, 2854, 1595, 1560, 1530, 1515, 1460, 1424, 1367, 1320, 1262, 1190, 1153, 1092, 1052, 1037; ^{1}H NMR (300 MHz, DMSO-*d*$_6$) δ: 1.74 (s, 3H, *CH*$_3$), 4.39 (d, *J* = 6 Hz, 2H, *CH*$_2$NH), 4.65 (t, *J* = 5.1 Hz, 2H, N*CH*$_2$), 4.78 (t, *J* = 5.1 Hz, 2H, N*CH*$_2$), 5.88 (t, *J* = 6 Hz, 1H, *NH*), 6.55-6.65 (m, 2H, Ar*H*), 7.05-7.10 (m, 1H, Ar*H*), 7.23 (d, *J* = 7.8 Hz, 1H, Ar*H*), 7.83 (s, 1H), 8.01 (s, 1H); ^{13}C NMR (100 MHz, DMSO-*d*$_6$) δ: 12.74, 38.28, 46.26, 48.70, 111.55, 116.81, 117.95, 123.60, 127.92, 128.93, 133.22, 138.33, 143.55, 145.96, 151.20; ESI-MS (*m/z*) calculated for $C_{15}H_{16}ClN_7O_2$: 361.10, found: 361.14 $[M]^+$, 363.12 $[M + 2]^+$; Anal. calcd. for $C_{15}H_{16}ClN_7O_2$: C, 49.80; H, 4.46; Cl, 9.80; N, 27.10; O, 8.84; found: C, 50.13; H, 4.69; Cl, 9.99; N, 27.27; O, 9.11.

5.5.30. 3-Chloro-N-((1-(2-(2-methyl-5-nitro-1H-imidazol-1-yl)ethyl)-1H-1,2,3-triazol-4-yl)methyl) aniline ***(32)*****:** Yield 60%; mp 101-102 ^{o}C; IR (KBr, cm^{-1}): 3382, 3112, 3075, 2851, 1599, 1528, 1461, 1424, 1367, 1323, 1262, 1190, 1154, 1086, 1051, 986; ^{1}H NMR (300 MHz, DMSO-*d*$_6$) δ: 1.76 (s, 3H, *CH*$_3$), 4.27 (d, *J* = 5.4 Hz, 2H, *CH*$_2$NH), 4.67 (d, *J* = 3.3 Hz, 2H, N*CH*$_2$), 4.79 (s, 2H, N*CH*$_2$), 6.45-6.60 (m, 3H, Ar*H*), 7.02-7.07 (m, 1H, Ar*H*), 7.86 (s, 1H), 8.02 (s, 1H); ESI-MS (*m/z*) calculated for $C_{15}H_{16}ClN_7O_2$: 361.10, found: 362.14 [M +

H]$^+$, 364.16 [M + 2]$^+$; Anal. calcd. for $C_{15}H_{16}ClN_7O_2$: C, 49.80; H, 4.46; Cl, 9.80; N, 27.10; O, 8.84; found: C, 50.07; H, 4.69; Cl, 9.95; N, 27.31; O, 8.98.

5.5.31. 4-Bromo-N-((1-(2-(2-methyl-5-nitro-1H-imidazol-1-yl)ethyl)-1H-1,2,3-triazol-4-yl)methyl) aniline ***(33)*****:** Yield 62%; mp 145-146 ^{o}C; IR (film, cm^{-1}): 3402, 3134, 3012, 1594, 1527, 1465, 1428, 1362, 1260, 1188, 1145, 1048, 818, 752; ^{1}H NMR (300 MHz, $CDCl_3$) δ: 1.93 (s, 3H, *CH_3*), 4.23 (brs, 1H, *NH*), 4.38 (d, *J* = 5.1 Hz, 2H, *CH_2*NH), 4.76 (s, 4H, N*CH_2CH_2*N), 6.49 (d, *J* = 8.8 Hz, 2H, Ar*H*), 7.12 (s, 1H), 7.25 (dd, *J* = 8, 1.4 Hz, 2H, Ar*H*), 7.97 (s, 1H); ESI-MS (*m/z*) calculated for $C_{15}H_{16}BrN_7O_2$: 405.05, found: 406.13 [M + H]$^+$, 408.17 [M + 2]$^+$; Anal. calcd. for $C_{15}H_{16}BrN_7O_2$: C, 44.35; H, 3.97; Br, 19.67; N, 24.14; O, 7.88; found: C, 44.66; H, 4.14; Br, 19.55; N, 24.66; O, 8.05.

5.5.32. 2,3-Dichloro-N-((1-(2-(2-methyl-5-nitro-1H-imidazol-1-yl)ethyl)-1H-1,2,3-triazol-4-yl) methyl)aniline ***(34)*****:** Yield 62%; mp 148-149 ^{o}C; IR (KBr, cm^{-1}): 3363, 3108, 2857, 1584, 1529, 1502, 1460, 1424, 1366, 1321, 1261, 1221, 1189, 1151, 1181, 1041, 899; ^{1}H NMR (300 MHz, DMSO-*d_6*) δ: 1.74 (s, 3H, *CH_3*), 4.42 (d, *J* = 5.7 Hz, 2H, *CH_2*NH), 4.65 (t, *J* = 4.5 Hz, 2H, N*CH_2*), 4.78 (t, *J* = 4.5 Hz, 2H, N*CH_2*), 6.29 (t, *J* = 5.7 Hz, 1H, CH_2*NH*), 6.59 (d, *J* = 8.4 Hz, 1H, Ar*H*), 6.79 (dd, *J* = 8.1, 1.2 Hz, 1H, Ar*H*), 7.05-7.11 (m, 1H, Ar*H*), 7.82 (s, 1H), 8.01 (s, 1H); ^{13}C NMR (100 MHz, DMSO-*d_6*) δ: 12.76, 38.40, 46.25, 48.71, 109.84, 115.61, 116.95, 123.64, 128.29, 131.61, 133.22, 138.32, 145.33, 145.63, 151.16; ESI-MS (*m/z*) calculated for $C_{15}H_{15}Cl_2N_7O_2$: 395.06, found: 396.18 [M + H]$^+$, 398.17 [M + 2]$^+$, 400.17 [M + 4]$^+$; Anal. calcd. for $C_{15}H_{15}Cl_2N_7O_2$: C, 45.47; H, 3.82; Cl, 17.90; N, 24.74; O, 8.08; found: C, 45.71; H, 3.93; Cl, 18.16; N, 24.98; O, 8.21.

5.5.33. 2,4,5-Trichloro-N-((1-(2-(2-methyl-5-nitro-1H-imidazol-1-yl)ethyl)-1H-1,2,3-triazol-4-yl) methyl)aniline ***(35)*****:** Yield 74%; mp 169-170 ^{o}C; IR (film, cm^{-1}): 3378 3113, 1581, 1528, 1463, 1428, 1363, 1264, 1191, 1149, 1047, 829, 754; ^{1}H NMR (400 MHz, $CDCl_3$) δ: 1.98 (s, 3H, *CH_3*), 4.45 (d, *J* = 5.1 Hz, 2H, *CH_2*NH), 4.79 (s, 4H, N*CH_2CH_2*N), 4.84 (t, *J* = 5.9 Hz, 1H, CH_2*NH*), 6.71 (s, 1H, Ar*H*), 7.18 (s, 1H), 7.35 (s, 1H, Ar*H*), 7.98 (s, 1H); ESI-MS (*m/z*) calculated for $C_{15}H_{14}Cl_3N_7O_2$: 429.02, found: 430.08 [M + H]$^+$, 432.11 [M + 2]$^+$, 434.09 [M + 4]$^+$, 436.21 [M + 6]$^+$; Anal. calcd. for $C_{15}H_{14}Cl_3N_7O_2$: C, 41.83; H, 3.28; Cl, 24.70; N, 22.77; O, 7.43; found: C, 42.11; H, 3.43; Cl, 24.69; N, 22.80; O, 7.58.

5.5.34. 3,5-Dimethoxy-N-((1-(2-(2-methyl-5-nitro-1H-imidazol-1-yl)ethyl)-1H-1,2,3-triazol-4-yl) methyl)aniline ***(36)*****:** Yield 69%; mp 136-138 ^{o}C; IR (film, cm^{-1}): 3397, 3131, 2956,

1605, 1528, 1465, 1364, 1262, 1197, 1151, 1055, 930, 817, 753; ^{1}H NMR (400 MHz, $CDCl_3$) δ: 1.95 (s, 3H, *CH*$_3$), 3.73 (s, 6H, 2*OCH*$_3$), 4.19 (brs, 1H, *NH*), 4.39 (s, 2H, *CH*$_2$NH), 4.76 (s, 4H, N*CH*$_2$*CH*$_2$N), 5.80 (d, *J* = 2 Hz, 2H, Ar*H*), 5.90-5.91 (m, 1H, Ar*H*), 7.16 (s, 1H), 7.98 (s, 1H); ESI-MS (*m/z*) calculated for $C_{17}H_{21}N_7O_4$: 387.16, found: 388.21 $[M + H]^+$; Anal. calcd. for $C_{17}H_{21}N_7O_4$: C, 52.71; H, 5.46; N, 25.31; O, 16.52; found: C, 52.87; H, 5.71; N, 25.52; O, 16.33.

5.5.35. N-((1-(2-(2-Methyl-5-nitro-1H-imidazol-1-yl)ethyl)-1H-1,2,3-triazol-4-yl)methyl) pyridine-2 amine ***(37):*** Yield 51%; mp 154-155 ^{o}C; IR (film, cm^{-1}): 3019, 1603, 1526, 1469, 1365, 1262, 1214, 1148, 1046, 745; ^{1}H NMR (300 MHz, DMSO-*d*$_6$) δ: 1.75 (s, 3H, *CH*$_3$), 4.41 (d, *J* = 5.1 Hz, 2H, NH*CH*$_2$), 4.64 (brs, 2H, N*CH*$_2$), 4.75 (brs, 2H, N*CH*$_2$), 6.45 (d, *J* = 6.9 Hz, 2H, Ar*H*), 6.92 (brs, 1H, *NH*), 7.31-7.36 (m, 1H, Ar*H*), 7.79 (s, 1H), 7.94 (s, 1H), 8.0 (s, 1H); ESI-MS (*m/z*) calculated for $C_{14}H_{16}N_8O_2$: 328.14, found: 328.19 $[M]^+$; Anal. calcd. for $C_{14}H_{16}N_8O_2$: C, 51.21; H, 4.91; N, 34.13; O, 9.75; found: C, 51.40; H, 5.22; N, 34.46; O, 10.03.

5.5.36. N-((1-(2-(2-Methyl-5-nitro-1H-imidazol-1-yl)ethyl)-1H-1,2,3-triazol-4-yl)methyl)-2-phenylethanamine ***(38):*** Yield 52%; mp 79-80 ^{o}C; IR (film, cm^{-1}): 3383, 3132, 3026, 1654, 1608, 1533, 1466, 1430, 1366, 1263, 1191, 1147, 1046, 825, 753; ^{1}H NMR (300 MHz, DMSO-*d*$_6$) δ: 1.86 (s, 3H, *CH*$_3$), 2.76 (brs, 3H), 3.86 (s, 4H, *CH*$_2$NH*CH*$_2$), 4.70-4.72 (m, 2H, N*CH*$_2$), 4.82 (s, 2H, N*CH*$_2$), 7.19-7.22 (m, 3H, Ar*H*), 7.26-7.29 (m, 2H, Ar*H*), 7.87 (s, 1H), 8.04 (s, 1H); ESI-MS (*m/z*) calculated for $C_{17}H_{21}N_7O_2$: 355.17, found: 355.15 $[M]^+$; Anal. calcd. for $C_{17}H_{21}N_7O_2$: C, 57.45; H, 5.96; N, 27.59; O, 9.00; found: C, 57.68; H, 6.13; N, 27.77; O, 9.25.

Acknowledgements

D.S.R. thanks SERB-Department of Science and Technology [EMR/2014/001127] New Delhi, India for financial support. D.K. and Beena are thankful to CSIR for the award of junior and senior research fellowship. Authors are also thankful to CIF-USIC, University of Delhi, Delhi for spectral data.

References

[1] Enright, M. C.; Robinson, D. A.; Randle, G.; Feil, E. J.; Grundmann, H.; Spratt, B. G. The evolutionary history of methicillin-resistant *Staphylococcus aureus* (MRSA). *Proc. Natl. Acad. Sci. USA* **2002**, *99*, 7687–7692.

[2] Tong, S. Y. C.; Varrone, L.; Chatfield, M. D.; Beaman, M.; Giffard, P. M. Progressive increase in community-associated methicillin resistant *Staphylococcus aureus* in Indigenous populations in northern Australia from 1993 to 2012. *Epidemiol. Infect.* **2015**, *143*, 1519–1523.

[3] Waness, A. Revisiting Methicillin-resistant *Staphylococcus aureus* infections. *J. Glob. Infect. Dis.* **2010**, *2*, 49–56.

[4] Archer, G. L. *Staphylococcus aureus*: a well-armed pathogen. *Clin. Infect. Dis.* **1998**, *26*, 1179–1181.

[5] David, M. Z.; Daum, R. S. Community-associated methicillin-resistant *Staphylococcus aureus*: epidemiology and clinical consequences of an emerging epidemic. *Clin. Microbiol. Rev.* **2010**, *23*, 616–687.

[6] Frazee, B. W.; Lynn, J.; Charlebois, E. D.; Lambert, L.; Lowery, D.; Perdreau-Remington, F. High prevalence of methicillin-resistant *Staphylococcus aureus* in emergency department skin and soft tissue infections. *Ann. Emerg. Med.* **2005**, *45*, 311–320.

[7] Klein, E.; Smith, D. L.; Laxminarayan, R. Hospitalizations and deaths caused by methicillin-resistant *Staphylococcus aureus*, United States, 1999-2005. *Emerg. Infect. Dis.***2007**, *13*, 1840–1846.

[8] Fraise, A. P. Tigecycline: The answer to beta-lactam and fluoroquinolone resistance? *J. Infect.* **2006**, *53*, 293–300.

[9] Critchley, I. A.; Blosser-Middleton, R. S.; Jones, M. E.; Thornsberry, C.; Sahm, D. F.; Karlowsky, J. A. Baseline study to determine *in vitro* activities of daptomycin against gram-positive pathogens isolated in the United States in 2000-2001. *Antimicrob. Agents Chemother.* **2003**, *47*, 1689–1693.

[10] Bouley, R.; Kumarasiri, M.; Peng, Z.; Otero, L. H.; Song, W.; Suckow, M. A.; Schroeder, V. A.; Wolter, W. R.; Lastochkin, E.; Antunes, N. T.; Pi, H.; Vakulenko, S.; Hermoso, J. A.; Chang, M.; Mobashery, S. Discovery of antibiotic (E)-3-(3-carboxyphenyl)-2-(4-cyanostyryl)quinazolin-4(3*H*)-one *J. Am. Chem. Soc.* **2015**, *137*, 1738–1741.

[11] Walsh, C.; Wright, G. Introduction: Antibiotic resistance. *Chem. Rev.* **2005**, *105*, 391–394.

[12] Fernandez, R.; Paz, L. I.; Rosato, R. R.; Rosato, A.E. Ceftaroline is active against hetero resistant methicillin-resistant *Staphylococcus aureus* clinical strains despite associated mutational mechanisms and intermediate levels of resistance. *Antimicrob. Agents Chemother.* **2014**, *58*, 5736–5746.

[13] Hiramatsu, K.; Katayama, Y.; Matsuo, M.; Sasaki, T.; Morimoto, Y.; Sekiguchi, A.; Baba, T. Multi-drug-resistant *Staphylococcus aureus* and future chemotherapy. *J. Infect. Chemother.* **2014**, *20*, 593–601.

[14] Kumarasamy, K. K.; Toleman, M. A.; Walsh, T.R.; Bagaria, J.; Butt, F.; Balakrishnan, R.; Chaudhary, U.; Doumith, M.; Giske, C. G.; Irfan, S.; Krishnan, P.; Kumar, A. V.; Maharjan, S.; Mushtaq, S.; Noorie, T.; Paterson, D. L.; Pearson, A.; Perry, C.; Pike, R.; Rao, B.; Ray, U.; Sarma, J. B.; Sharma, M.; Sheridan, E.; Thirunarayan, M. A.; Turton, J.; Upadhyay, S.; Warner, M.; Welfare, W.; Livermore, D. M.; Woodford, N. Emergence of a new antibiotic resistance mechanism in India, Pakistan, and the UK: A molecular, biological, and epidemiological study. *Lancet Infect. Dis.* **2010**, *10*, 597–602.

[15] Bush, K.; Courvalin, P.; Dantas, G.; Davies, J.; Eisenstein, B.; Huovinen, P.; Jacoby, G. A.; Kishony, R.; Kreiswirth, B.N.; Kutter, E.; Lerner, S.A.; Levy, S.; Lewis, K.; Lomovskaya, O.; Miller, J. H.; Mobashery, S.; Piddock, L. J.; Projan, S.; Thomas, C. M.; Tomasz, A.; Tulkens, P. M.; Walsh, T. R.; Watson, J. D.; Witkowski, J.; Witte, W.; Wright, G.; Yeh, P.; Zgurskaya, H. I. Tackling antibiotic resistance. *Nat. Rev. Microbiol.* **2011**, *9*, 894–896.

[16] Arias, C. A.; Murray, B. E. Antibiotic-resistant bugs in the 21st centuryea clinical super-challenge. *New Engl. J. Med.* **2009**, *360*, 439-443.

[17] Matsuhashi, M.; Song, M. D.; Ishino, F.; Wachi, M.; Doi, M.; Inoue, M.; Ubukata, K.; Yamashita, N.; Konno, M. Molecular cloning of the gene of a penicillin-binding protein supposed to cause high resistance to β-lactam antibiotics in *Staphylococcus aureus*. *J Bacteriol.* **1986**, *167*, 975-980.

[18] Ito, T.; Katayama, Y.; Hiramatsu, K. Cloning and nucleotide sequence determination of the entire mecA DNA of pre-methicillin-resistant *Staphylococcus aureus* N315. *Antimicrob. Agents Chemother.* **1999**, *43*, 1449–1458.

[19] Lovering, A. L.; Gretes, M. C.; Safadi, S. S.; Danel, F.; de Castro, L.; Page, M. G. P.; Strynadka, N. C. J. Structural insights into the anti-methicillin-resistant *Staphylococcus aureus* (MRSA) activity of ceftobiprole. *The J. Biolog. Chem.* **2012**, *287*, 32096–32102.

[20] Otero, L. H.; Rojas-Altuve, A.; Llarrull, L. I.; Carrasco-López, C.; Kumarasiri, M.; Lastochkin, E.; Fishovitz, J.; Dawley, M.; Hesek, D.; Lee, M.; Johnson, J. W.; Fisher, J. F.; Chang, M.; Mobashery, S.; Hermoso, J. A. How allosteric control of *Staphylococcus aureus* penicillin binding protein 2a enables methicillin resistance and physiological function. *Proc. Natl. Acad. Sci. U S A.* **2013**, *110*, 16808–16813.

[21] Fishovitz, J.; Rojas-Altuve, A.; Otero, L. H.; Dawley, M.; Carrasco-Lopez, C.; Chang, M.; Hermoso, J. A.; Mobashery, S. Disruption of allosteric response as an unprecedented mechanism of resistance to antibiotics. *J. Am. Chem. Soc.* **2014**, *136*, 9814−9817.

[22] Acebrón, I.; Chang, M.; Mobashery, S.; Hermoso, J. A. The allosteric site for the nascent cell wall in penicillin-binding protein 2a: An Achilles' Heel of methicillin-resistant *Staphylococcus aureus*. *Curr. Med. Chem.* **2015**, *22*, 1678-1686.

[23] Lofmark, S.; Edlund, C.; Nord, C. E. Metronidazole is still the drug of choice for treatment of anaerobic infections. *Clin. Infect. Dis.* **2010**, *50*, S16–23.

[24] Cui, S. F.; Peng, L. P.; Zhang, H. Z.; Rasheed, S.; Kumar, K. V.; Zhou, C. H. Novel hybrids of metronidazole and quinolones: Synthesis, bioactive evaluation, cytotoxicity, preliminary antimicrobial mechanism and effect of metal ions on their transportation by human serum albumin. *Eur. J. Med. Chem.* **2014**, *86*, 318–334.

[25] Duan, Y. T.; Wang, Z. C.; Sang, Y. L.; Tao, X. X.; Teraiya, S. B.; Wang, P. F.; Wen, Q.; Zhou, X. J.; Ding, L.; Yang, Y. H.; Zhu, H. L. Design and synthesis of 2-styryl of 5-nitroimidazole derivatives and antimicrobial activities as FabH inhibitors *Eur. J. Med. Chem.* **2014**, *76*, 387–396

[26] Wang, S. F.; Yin, Y.; Qiao, F.; Wu, X.; Sha, S.; Zhang, L.; Zhu, H. L. Synthesis, molecular docking and biological evaluation of metronidazole derivatives containing piperazine skeleton as potential antibacterial agents. *Bioorg. Med. Chem.* **2014**, *22*, 2409–2415.

[27] Hu, W.; Burli, R. W.; Kaizerman, J. A.; Johnson, K. W.; Gross, M. I.; Iwamoto, M.; Jones, P.; Lofland, D.; Difuntorum, S.; Chen, H.; Bozdogan, B.; Appelbaum, P. C.; Moser, H. E. DNA binding ligands with improved in vitro and in vivo potency against drug-resistant *Staphylococcus aureus. J. Med. Chem.* **2004**, *47*, 4352–4355

[28] Hu, X. L.; Li, D.; Shao, L.; Dong, X.; He, X. P.; Chen, G. R.; Chen, D. Triazole-linked glycolipids enhance the susceptibility of MRSA to β-lactam antibiotics. *ACS Med. Chem. Lett.* **2015**, *6*, 793−797

[29] Beena; Kumar, N.; Rohilla, R. K.; Roy, N.; Rawat, D. S. Synthesis and antibacterial activity evaluation of metronidazole-triazole conjugates. *Bioorg. Med. Chem. Lett.* **2009**, *19*, 1396–1398.

[30] Negi, B.; Raj, K. K.; Siddiqui, S. M.; Ramachandran, D.; Azam, A.; Rawat, D. S. *In vitro* antiamoebic activity evaluation and docking studies of metronidazole–triazole hybrids. *Chem. Med. Chem.* **2014,** *11*, 2439–2444.

[31] Beena; Kumar, D.; Bailey, M. A.; Parish, T.; Rawat, D. S. Synthesis and antituberculosis activity evaluation of cyclohexane-1,2-diamine derivatives. *Chem. Biol. Interface.* **2014**, *4*, 1–14.

[32] Beena; Kumar, D.; Kumbukgolla, W.; Jayaweera, S.; Bailey, M. A.; Alling, T.; Ollinger, J.; Parish, T.; Rawat, D. S. Antibacterial activity of adamantyl substituted cyclohexane diamine derivatives against methicillin resistant *Staphylococcus aureus* and *Mycobacterium tuberculosis*. *RSC advances*. **2014**, *4*, 11962–11966.

[33] Kumar, D.; Raj, K. K.; Bailey, M. A.; Alling, T.; Parish, T.; Rawat, D. S. Antimycobacterial activity evaluation, time-kill kinetic and 3D-QSAR study of C-(3-aminomethyl-cyclohexyl)-methylamine derivatives. *Bioorg. Med. Chem. Lett.* **2013**, *23* 1365–1369.

[34] Beena; Joshi, S.; Kumar, N.; Kidwai, S.; Singh, R.; Rawat, D. S. Synthesis and antitubercular activity evaluation of novel unsymmetrical cyclohexane-1,2-diamine derivatives. *Arch. Pharm. Chem. Life Sci.* **2012**, *345*, 896–901.

[35] Kumar, D.; Beena; Khare, G.; Tyagi, A. K.; Singh, R.; Rawat, D. S. Synthesis of novel 1,2,3-triazole derivatives of isoniazid and their *in vitro* antimycobacterial activity evaluation. *Eur. J. Med. Chem.* **2014**, *81*, 301–313.

[36] Knight, R. C.; Skolimowski, I. M.; Edwards, D. I., The interaction of reduced metronidazole with DNA. *Biochem. Pharmacol.,* **1978,** *27*, 2089-2093.

[37] Tocher, J. H.; Edwards, D. I., Evidence for the direct interaction of reduced metronidazole derivatives with DNA bases. *Biochem. Pharmacol.,* **1994,** *48*, 1089-1094.

[38] Pick, N.; Cameron, S.; Arad, D.; Av-Gay, Y. Screening of compounds toxicity against human monocytic cell line-THP-1 by flow cytometry. *Biol. Proced. Online*. **2004**, *6*, 220–225.

[39] Garcia, I.; Pouzet, C.; Brulas, M.; Bauza, E.; Botto, J.M.; Domloge, N. Evaluation of THP-1 cell line as an *in vitro* model for long-term safety assessment of new molecules. *Int. J. Cosmet. Sci.* **2013**, *35*, 568–574.

[40] Lim, D.; Strynadka, N. C. Structural basis for the beta lactam resistance of PBP2a from methicillin-resistant *Staphylococcus aureus*. *Nat. Struct. Biol.* **2002**, *9*, 870–876.

[41] QikProp User Manual Copyright © 2013 Schrödinger, LLC.

[42] Lu, J. J.; Crimin, K.; Goodwin, J. T.; Crivori, P.; Orrenius, C.; Xing, L.; Tandler, P. J.; Vidmar, T. J.; Amore, B. M.; Wilson, A. G. E.; Stouten, P. F. W.; Burton, P. S. Influence of molecular flexibility and polar surface area metrics on oral bioavailability in the rat. *J. Med.Chem.* **2004**, *47*, 6104–6107.

[43] Artursson, P.; Palm, K.; Luthman, K. Caco-2 monolayers in experimental and theoretical predictions of drug transport. *Adv. Drug. Deliv. Rev.* **2001**, *46*, 27–43.

[44] Glide 5.8 User Manual Copyright © 2013 Schrödinger, LLC.

Table 1: *In Vitro* Anti-MRSA Activity of MTZ-Triazole Hybrids

Compound	R	MIC (μg/mL)						
		>128	**128**	**64**	**32**	**16**	**8**	**4**
4	CH_2Br	13	-	1	3	10	2	1
5	CH_2OCOEt	18	-	5	7	-	-	-
6	CH_2OTHP	14	-	1	2	10	3	-
7	TMS	6	-	24	-	-	-	-
8	$CH_2CH_2CH_3$	6	-	24	-	-	-	-
9	Cyclohexan-1-ol	6	-	24	-	-	-	-
10	Ph	12	-	1	0	9	8	-
11	CH_2OPh	4	-	18	1	1	3	3
12	CH_2OCH_3	16	-	2	4	4	3	-
13	CH_2OPh-4-CH_3	9	-	13	8	-	-	-
14	CH_2OPh-4-*i*Pr	6	-	24	-	-	-	-
15	CH_2OPh-4-*t*-Bu	6	-	24	-	-	-	-
16	CH_2OPh-2-CHO	6	-	24	-	-	-	-
17	CH_2O-4-CHOPh	14	-	7	3	5	1	-
18	CH_2OPh-2-Cl	6	-	24	-	-	-	-
19	CH_2OPh-4-NO_2	6	-	24	-	-	-	-
20	CH_2OPh-2,3-Me	6	-	24	-	-	-	-
21	CH_2OPh-2,4-Cl	6	-	24	-	-	-	-
22	CH_2OPh-2,6-Cl	7	2	5	5	1	1	9
23	CH_2OCH_2Ph	6	-	24	-	-	-	-
24	CH_2OPh-2,4,6-*t*-Bu	6	-	24	-	-	-	-
25	CH_2O-1-napthyl	12	-	1	3	8	5	1
26	CH_2NHPh	6	-	24	-	-	-	-
27	CH_2NHPh-2-CH_3	6	-	24	-	-	-	-
28	CH_2NHPh-2-F	5	-	8	0	12	4	1
29	CH_2NHPh-3-F	15	-	14	0	1	-	-
30	NHPh-4-F	7	-	23	-	-	-	-
31	CH_2NHPh-2-Cl	7	1	6	6	5	5	-
32	CH_2NHPh-3-ClPh	15	-	14	1	-	-	-
33	CH_2NHPh-4-Br	7	1	15	5	2	-	-
34	CH_2NHPh-2,3-Cl	15	-	14	-	1	-	-
35	CH_2NH-2,4,5-ClPh	6	-	24	-	-	-	-
36	NHPh-3,5-OMe	15	-	14	0	1	-	-

37	2-Aminopyridyl	6	-	24	-	-	-	-
38	$NHCH_2CH_2Ph$	15	-	14	0	1	-	-
Oxacillin		20	1	4	4	1	-	-

Table 2: Synergistic Activity of Compound 22 with Oxacillin Against MRSA

MRSA strains*	MIC (µg/mL)		
	Oxacillin	**Compound 22**	**Compound 22: Oxacillin (1:1)**
1a	>128	4	1
2a	>128	4	1
3a	>128	4	1
4a	>128	4	2
5a	>128	4	1
6a	>128	4	1
7a	>128	4	1
8a	>128	4	1
9a	>128	8	2
10a	>128	>128	2
11a	>128	16	1
12a	>128	32	2
13a	>128	64	4
14a	>128	>128	4
15a	>128	>128	4
16a	>128	32	2
17a	>128	32	1
18a	>128	32	4
19a	>128	32	2
20a	>128	>128	2
21a	64	4	1
22a	32	>128	4
23a	64	>128	4
24a	16	>128	4
25a	64	64	4
26a	32	64	4
27a	32	64	4
28a	128	128	1
29a	32	128	4
30a	64	64	8

*MRSA strains were isolated using axilla and nasal swabs obtained from Medical Students and Patients at Teaching Hospital Anuradhapura, Sri Lanka.

Table 3: Time dependent kill kinetics study of the compound 22 (32 µg/mL) against MRSA strain-1a

Incubation time (h)	Log_{10}CFU/mL Control Mean ± SD	Log_{10}CFU/mL Oxacillin Mean ± SD	Log_{10}CFU/mL NTZ Mean ± SD	Log_{10}CFU/mL Compd 22 Mean ± SD	Log_{10}CFU/mL Compd 22+OX Mean ± SD
0	5. 28 ± 0.417	5.28 ± 0.417	5.28 ± 0.417	5.28 ± 0.417	5. 28 ± 0.417
4	6.14 ±0.456	6.05 ±0.463	5.91±0.328	5.65± 0.47	5.50±0.456
8	8.30± 0.442	7.62±0.484	6.45±0.377	6.05±0.456	5.85±0.442
12	10.12±0.428	8.35±0.442	8.01±0.214	5.96±0.235	5.91±0.428
16	12.50±0.291	11.20±0.335	8.25±0.21	5.53±0.256	4.52±0.331
20	12.73±0.223	11.95±0.29	8.14±0.223	5.57±0.245	5.26±0.29
24	12.64±0.224	12.34±0.23	8.30±0.221	5.84±0.213	5.60±0.28

Table 4: Glide Docking Scores (kcal mol^{-1}) and Docking Energies of Best Active MTZ-Triazole Hybrids along with the Oxacillin and Metronidazole, bound to MRSA PBP2a Binding Site

Entry	Glide XP G Score	Glide Energy	Entry	Glide XP G Score	Glide Energy
4	-5.950	-43.558	25	-7.293	-55.457
10	-5.968	-44.869	28	-6.345	-48.259
11	-6.596	-53.285	OXA	-6.974	-52.099
12	-5.520	-40.322	MTZ	-5.389	-32.147
22	-6.323	-49.945			

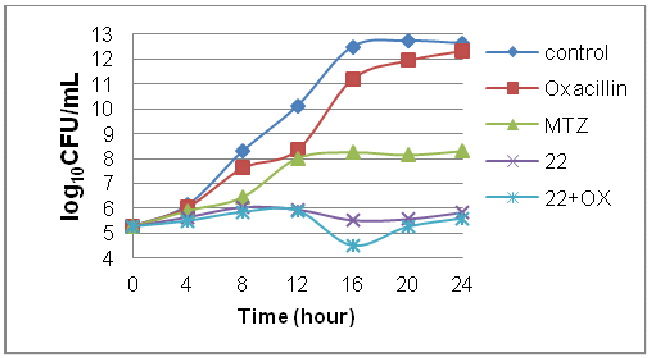

Figure 1: Graphical representation of Time dependent kill kinetics study of the compound **22** (32 µg/mL) against MRSA strain-1a

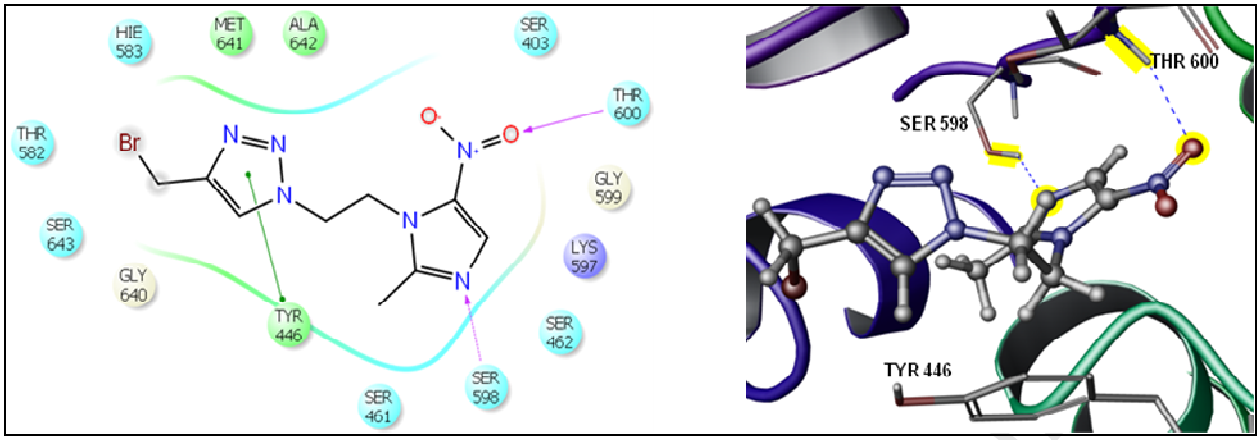

Figure 2: 2D and 3D docking pose showing interaction for compound **4** in the binding site of *S. aureus* PBP2a crystal structure (PDB ID:3ZFZ) from MRSA.

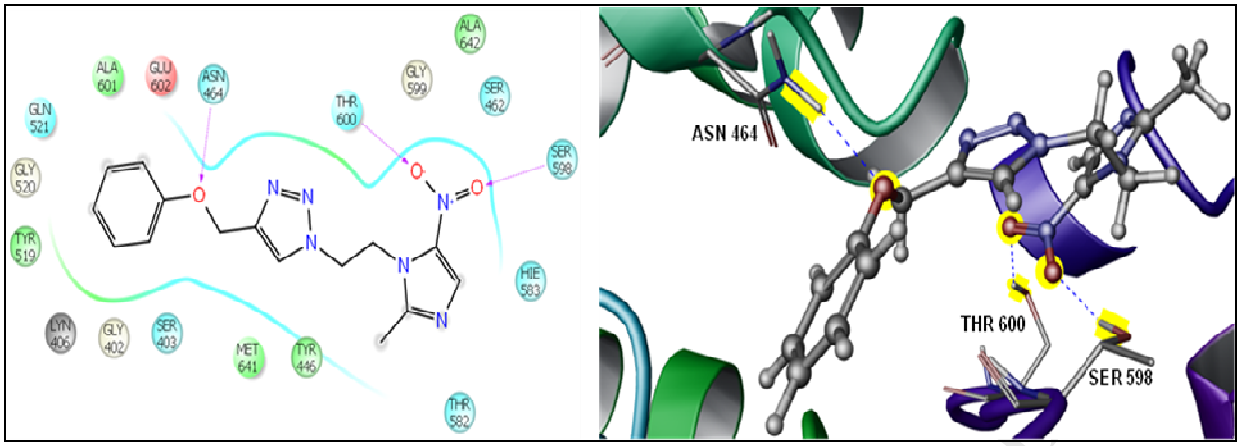

Figure 3: 2D and 3D docking pose showing interaction for compound **11** in the binding site of *S. aureus* PBP2a crystal structure (PDB ID:3ZFZ) from MRSA.

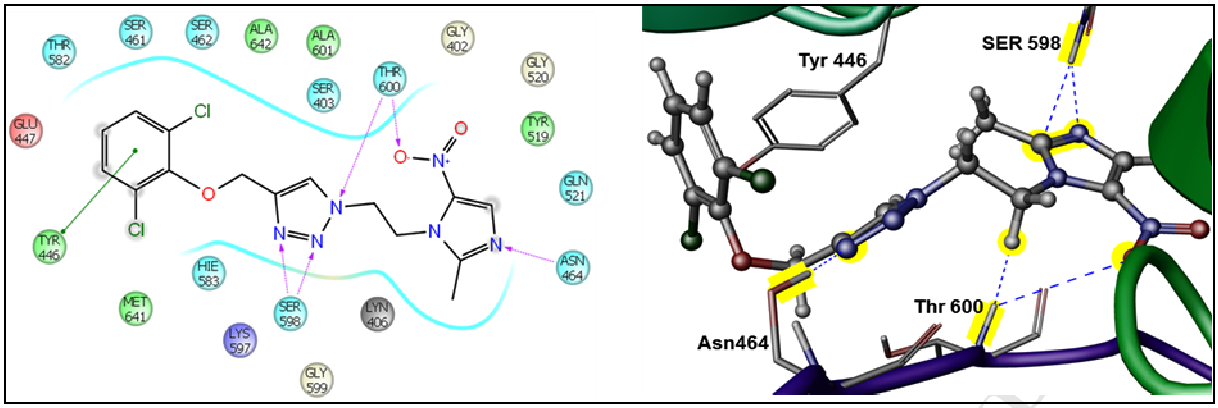

Figure 4: 2D and 3D docking pose showing interaction for compound **22** in the binding site of *S. aureus* PBP2a crystal structure (PDB ID:3ZFZ) from MRSA

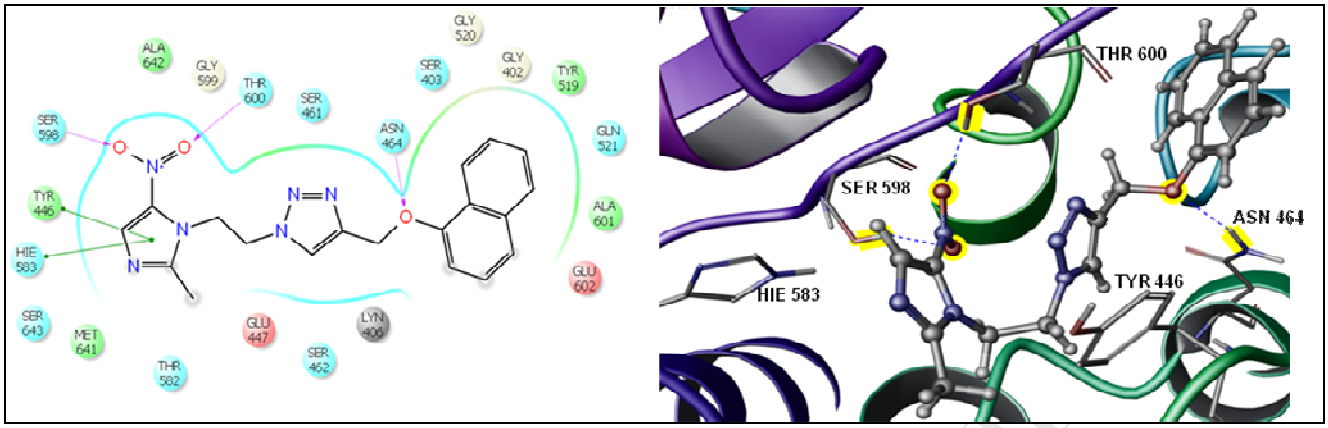

Figure 5: 2D and 3D docking pose showing interaction for compound **25** in the binding site of *S. aureus* PBP2a crystal structure (PDB ID:3ZFZ) from MRSA.

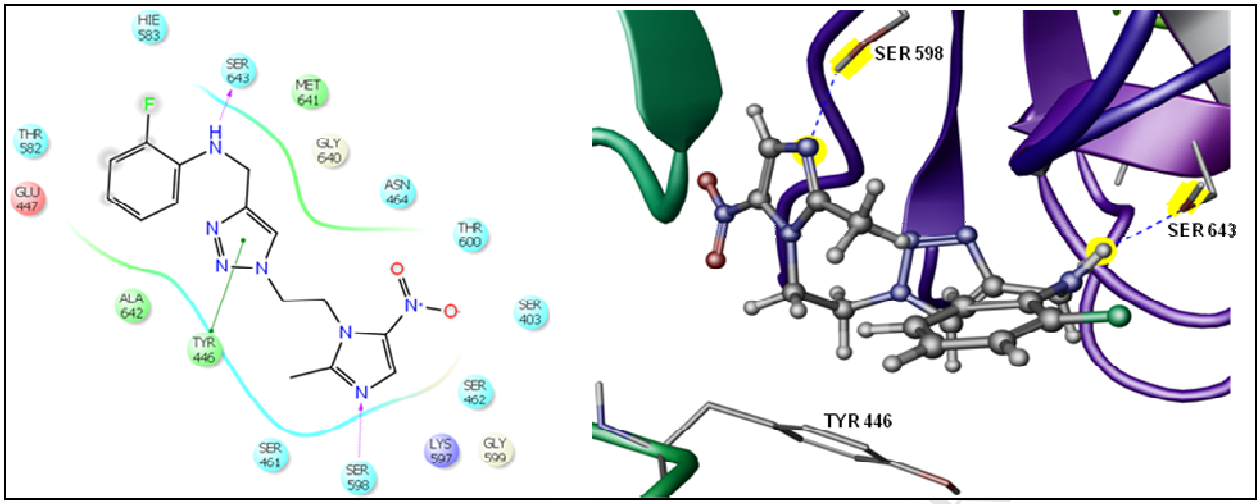

Figure 6: 2D and 3D docking pose showing interaction for compound **28** in the binding site of *S. aureus* PBP2a crystal structure (PDB ID:3ZFZ) from MRSA.

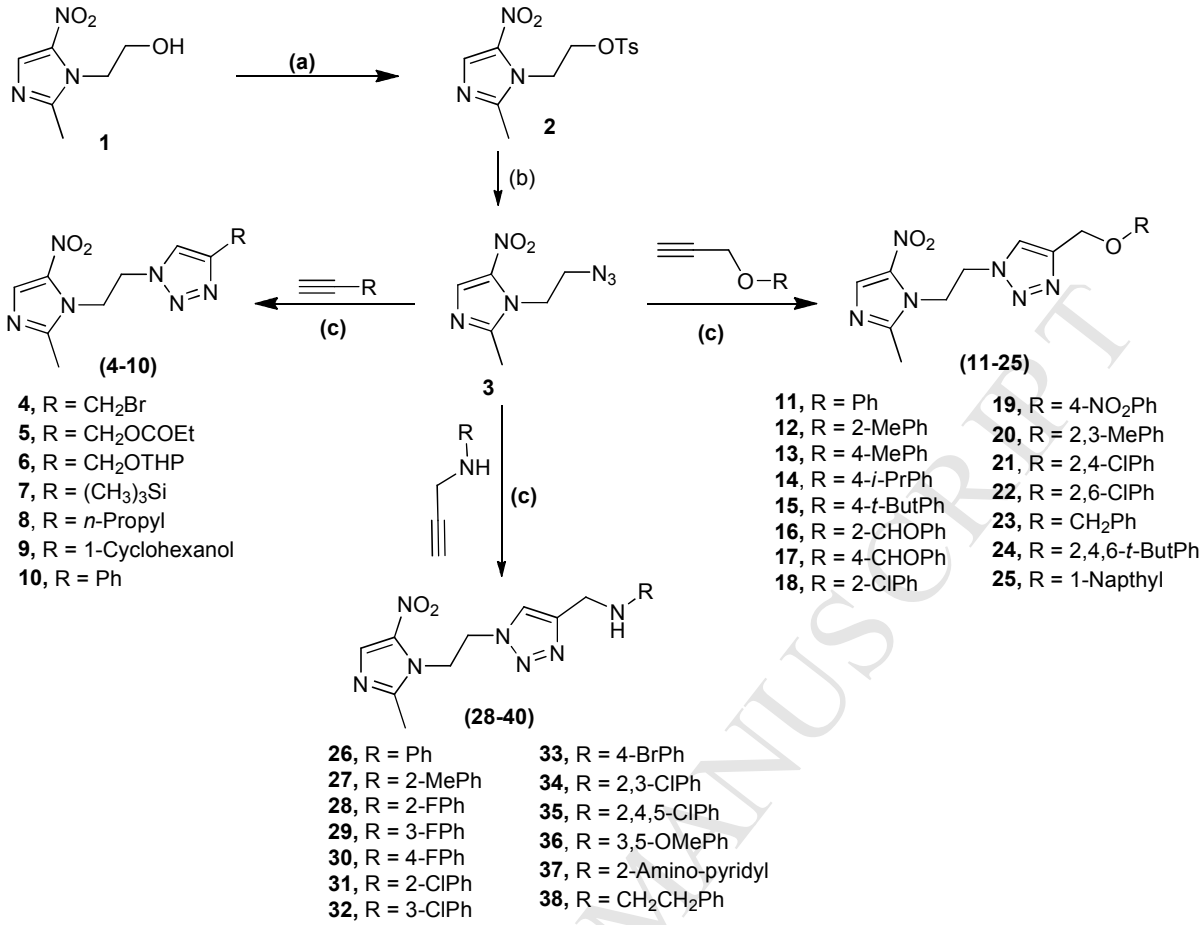

Reagents and conditions: (a) *p*-TsCl, Pyridine, RT, 12 h; (b) NaN_3, DMF at 0 ^oC then 70–80 ^oC for 1 h; (c) *t*-BuOH : H_2O (1:1) , Sodium ascorbate, $CuSO_4.5H_2O$, 51-75 %

Scheme 1: Synthesis of Metronidazole-Triazole Hybrids

Highlights

- *In vitro* anti-MRSA activity of a series of 35 metronidazole-triazole hybrids was reported against 30 different MRSA strains.
- One compound evaluated along with oxacillin and showed synergistic activity.
- Compounds were nontoxic up to 50 μM concentration against THP-1 cell lines.
- The time-kill kinetics studies suggested the compounds to be bacteriostatic.
- In silico studies, compounds showed good docking scores and pharmacokinetic properties and follow the Lipinski's rule of 5.